



# ANALYSIS OF THE BTZ BLACK HOLE

Properties of a  $(2+1)$  dimensional black hole solution

BACHELOR PROJECT IN PHYSICS

Written by *Christain Schiøtt and Rasmus Nielsen*

Monday 17<sup>th</sup> July, 2023

Supervised by

Poul Henrik Damgaard and Subodh Patil

UNIVERSITY OF COPENHAGEN



UNIVERSITY OF  
COPENHAGEN

NAME OF INSTITUTE: Niels Bohr Institutet

NAME OF DEPARTMENT: Niels Bohr International Academy

AUTHOR(S): Christain Schiøtt and Rasmus Nielsen

EMAIL: bcn852@alumni.ku.dk and jbz701@alumni.ku.dk

TITLE AND SUBTITLE: Analysis of the BTZ Black Hole  
- Properties of a (2+1) dimensional black hole solution

SUPERVISOR(S): Poul Henrik Damgaard and Subodh Patil

HANDED IN: 13.06.2018

DEFENDED: To be decided

NAME \_\_\_\_\_

SIGNATURE \_\_\_\_\_

DATE \_\_\_\_\_

## Abstract

Since Einstein proposed his theory of general relativity in 1915 physicists have searched for black hole solutions of all kinds. In 1992, Máximo Bañados, Claudio Teitelboim, and Jorge Zanelli discovered one such solution in a (2+1) dimensional spacetime with negative curvature called the BTZ Black Hole. In this thesis we construct the BTZ Black Hole from  $\text{AdS}_3$  and analyse its properties. We derive the metric and find that the rotating BTZ black hole possesses an inner and an outer event horizon at  $r_{\pm}^2 = \frac{\ell^2}{2} \left[ M \pm \sqrt{M^2 - \left(\frac{J}{\ell}\right)^2} \right]$ , where  $M$  and  $J$  are the mass and angular momentum of the black hole respectively, and  $\ell$  is related to the cosmological constant by  $\Lambda = -\ell^{-2}$ . This is very similar to the (3+1) dimensional Kerr Black Hole. We also find that apart from the behaviour at infinity, the causal structure of the static BTZ Black Hole resembles that of the Schwarzschild black hole quite closely.

Lastly, following the approach of [4] closely, we utilise that the static BTZ Black Hole can be constructed by a identification of points in 3 dimensional anti-de Sitter space, allowing for the exact computation of Green's functions on the static BTZ spacetime. Using the KMS condition, we show that the properties of these Green's functions are exactly those of a thermal Green's function, implying that the static BTZ Black Hole has a non-zero temperature of  $T = \frac{r_+}{2\pi\ell^2}$ .

## Resumé

Siden Einstein fremførte sin teori om generel relativitetsteori i 1915 har fysikere søgt efter løsninger der opfører sig som sorte huller. I 1992 opdagede Máximo Bañados, Claudio Teitelboim, and Jorge Zanelli en sådan løsning i en (2+1) dimensionel rumtid med negativ krumning kaldet et BTZ sort hul. I dette bachelorprojekt konstrueres det BTZ sorte hul ud fra  $\text{AdS}_3$  og det egenskaber analyseres. Vi udleder metrikken og ser at det roterende BTZ sorte hul besidder både en indre og en ydre begivenhedshorisont ved  $r_{\pm}^2 = \frac{\ell^2}{2} \left[ M \pm \sqrt{M^2 - \left(\frac{J}{\ell}\right)^2} \right]$ , hvor  $M$  og  $J$  er henholdsvis massen og det angulære moment af det sorte hul, og  $\ell$  er relateret til den kosmologiske konstant ved  $\Lambda = -\ell^{-2}$ . Dette er meget lig det (3+1) dimensionale Kerr sorte hul. Vi finder desuden, at på nær opførelsen ved uendelig, at den kausale struktur af det statiske BTZ sorte hul har mange ligheder med den kausale struktur af Schwarzschild sorte huller.

Til slut følger vi udledningen givet i [4] tæt og udnytter, at det statiske BTZ sorte hul kan konstrueres ved identifikation af punkter i 3 dimensionalt anti-de Sitter space, hvilket muliggør en eksakt udregning af Green's funktioner på den statiske BTZ rumtid. Ved brug af KMS betingelsen vises det, at disse Green's funktioner har præcis de egenskaber vi forventer for en termisk Green's funktion, hvilket medfører at det statiske BTZ sorte hul har temperaturen  $T = \frac{r_+}{2\pi\ell^2}$ .

# Contents

<b>1</b>	<b>Introduction</b>	<b>1</b>
1.1	Black hole solutions . . . . .	1
1.1.1	The Schwarzschild Black Hole . . . . .	1
1.1.2	No-hair Theorem and the Information Paradox . . . . .	3
1.1.3	The Kerr Black Hole . . . . .	3
1.2	Aspects of QFT on curved backgrounds . . . . .	5
1.2.1	The Unruh Effect . . . . .	5
1.3	Gravity in (2+1) dimensions . . . . .	6
<b>2</b>	<b>Derivation of the BTZ metric</b>	<b>8</b>
2.1	An ansatz for the Einstein Equations . . . . .	8
2.2	Solving the Einstein Equations . . . . .	8
2.3	Connection to anti-de Sitter space . . . . .	12
2.3.1	Anti-de Sitter space . . . . .	12
2.3.2	Constructing the BTZ spacetime . . . . .	13
<b>3</b>	<b>Classical properties of the BTZ spacetime</b>	<b>14</b>
3.1	Causal structure of the spacetime . . . . .	14
3.2	Singularities . . . . .	19
<b>4</b>	<b>Quantum fields on fixed BTZ background</b>	<b>20</b>
4.1	KMS condition and the two-point function . . . . .	20
4.1.1	Computing the AdS Green's functions . . . . .	21
4.1.2	Computing the BTZ Green's functions . . . . .	23
4.1.3	The KMS condition . . . . .	24
<b>5</b>	<b>Conclusion</b>	<b>25</b>
<b>A</b>	<b>The basics of General Relativity</b>	<b>26</b>
A.1	Differential Forms . . . . .	26
A.2	The metric . . . . .	26
A.3	Covariant Derivatives and Connections . . . . .	26
A.4	Curvature of the spacetime . . . . .	27
A.5	Geodesics . . . . .	27
A.6	Einstein's Equation . . . . .	27
A.7	Killing vectors and symmetries . . . . .	28
A.8	Kruskal and Penrose Diagrams . . . . .	28
<b>B</b>	<b>BTZ parameterization of AdS3</b>	<b>29</b>

# 1 Introduction

In this thesis, we set out to investigate the properties of the (2+1) dimensional black hole solution, discovered by **Máximo Bañados**, **Claudio Teitelboim**, and **Jorge Zanelli**, known as the **BTZ black hole**. Our aim is to first discuss the properties of the solution from the perspective of classical general relativity, of which a brief review is located in appendix A. Following that, we aim to investigate the consequences of having the BTZ spacetime be the background of a quantum scalar field theory. As will be shown, the BTZ Green's functions (sometimes referred to as two-point functions) will obey the KMS condition and the black hole will have a non-zero temperature, as is also the case for the Schwarzschild black hole. The structure of the thesis will be as follows:

In **section 1**, we will first introduce the basic concepts of event horizons and black holes. We will then discuss the properties of some black hole solutions in (3+1) dimensions. Following that, some general features of quantum field theory in curved spaces are discussed. Lastly, we will go over the general features of standard general relativity in (2+1) dimensions.

In **section 2**, we derive the BTZ metric by solving the **Einstein Equations** in (2+1) dimensions, assuming the existence of a time-like and a space-like **Killing vector**. We then discuss how the BTZ spacetime can be obtained by identifying certain points of the 3 dimensional **anti-de Sitter spacetime**.

In **section 3**, we investigate the causal structure of the maximally extended static BTZ spacetime. We also discuss the nature of the singularities of the BTZ spacetime, and the existence of **closed time-like curves** under a specific extension of the spacetime.

In **section 4**, we first discuss the **KMS condition** and how it implies that periodicity in imaginary time of the scalar field two-point functions give rise to a non-zero temperature. We then compute the two-point functions on  $AdS_3$ , and connect them to those of the static BTZ spacetime through the method of images. Lastly, we demonstrate that the static BTZ Green's functions obey the KMS condition, implying a non-zero temperature for the static BTZ black hole.

## 1.1 Black hole solutions

The popular idea of a black hole is something all-devouring, something so massive that it is impossible to escape its gravitational pull. A physicist's idea of a black hole is not too far from that image, but to give a proper definition of a black hole, we must first define the concept of an event horizon:

**Definition 1.1. Event Horizons:** The (*future / past*) event horizon of an asymptotically maximally symmetric spacetime, is the boundary of the causal (*past / future*) of conformal infinity  $\mathcal{J}$ . The causal (*past / future*) of conformal infinity is denoted  $J^\pm(\mathcal{J})$ .

A **black hole** is then simply defined as  $\mathcal{M} \setminus J^-(\mathcal{J})$ , where  $\mathcal{M}$  is the entire spacetime. This means that any future-directed timelike world line that goes into the black hole is unable to reach null infinity, which is what gives rise to the popular interpretation of black holes that a black hole is something you can not escape.

### 1.1.1 The Schwarzschild Black Hole

The simplest and most well-known black hole solution is the Schwarzschild black hole in (3+1)-dimensions, with the Schwarzschild metric written in Schwarzschild coordinates as:

$$ds^2 = -\left[1 - \frac{2GM}{r}\right] dt^2 + \left[1 - \frac{2GM}{r}\right]^{-1} dr^2 + r^2 d\Omega_2^2 \quad (1.1)$$

$$t \in (-\infty, \infty) \quad , \quad r \in (0, 2GM) \cup (2GM, \infty) \quad (1.2)$$

In the above metric,  $d\Omega_2^2$  stands for the metric of a 2-sphere in the usual spherical coordinates. This metric has an apparent singularity at  $r = 2GM$ , but a change of coordinates reveals that it is only a

coordinate singularity. The only real singularity is at  $r = 0$  where the curvature invariant  $R_{\rho\sigma\mu\nu} R^{\rho\sigma\mu\nu}$  becomes infinite. One set of coordinates in which this can be seen is the Kruskal–Szekeres coordinates in which the metric takes the form:

$$ds^2 = \frac{32 G^3 M^3}{r} e^{r/2GM} (-dT^2 + dX^2) + r^2 d\Omega_2^2, \quad T^2 - X^2 < 1 \quad (1.3)$$

In the above  $r$  is regarded as an implicit function of  $X$  and  $T$ . Switching to these coordinates not only reveals the non-singular nature of the event horizon, it also reveals another curious fact about the spacetime: The traditional Schwarzschild coordinates do not cover the entire spacetime. When switching to Kruskal-Szekeres coordinates, it is possible to follow geodesics to extend the spacetime into a geodesically complete spacetime; a spacetime in which no geodesics stop at finite parameter value. Two diagrams are used to study the causal structure of this maximally extended spacetime; the **Kruskal diagram** and the **Conformal diagram**.

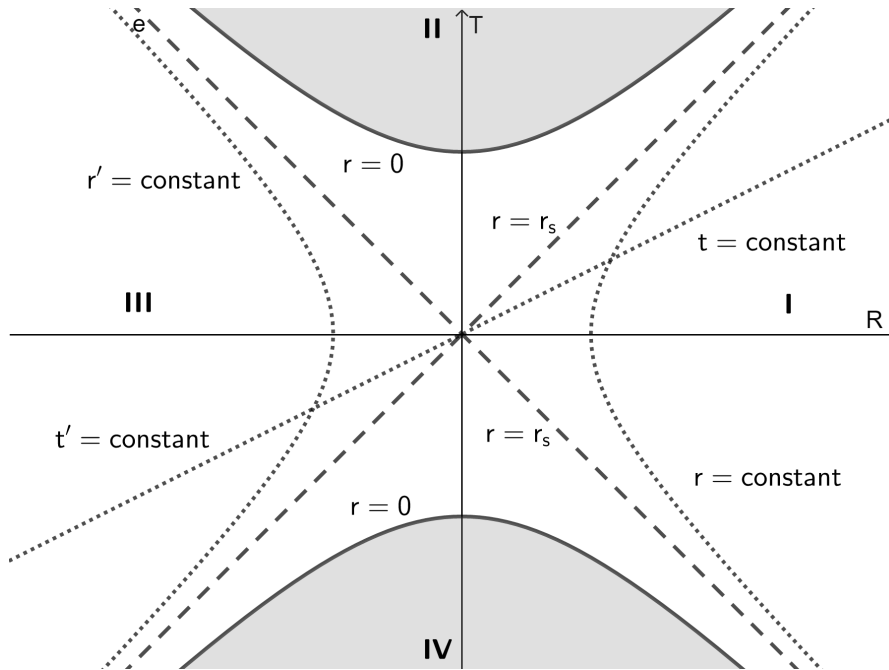


Figure 1: Kruskal diagram for the maximally extended Schwarzschild spacetime. The event horizon is located at  $r = r_s$ , while the curvature singularity is located at  $r = 0$ . The grey areas above and below the  $r = 0$  curves are not part of the spacetime.

The Kruskal diagram shows the spacetime in the Kruskal-Szekeres coordinates, where light cones stand upright and at  $45^\circ$  everywhere, as can easily be seen from (1.3). The event horizon at  $r = r_s$  naturally separates the spacetime into four regions. The regions I and III are two disconnected (*meaning not connected by future- or past-directed causal curves*) regions. The region II is the black hole, where hitting the singularity at  $r = 0$  is unavoidable following any future-directed timelike path. The most surprising region IV, is called the white hole, and is the time-reversed version of the black hole. This means that all past-directed timelike paths in region IV, must hit the singularity at  $r = 0$ , or equivalently that it is impossible to enter the white hole from region I or III.

The Conformal diagram shows the spacetime in a set of compact coordinates, such that the nature of the infinities becomes more apparent. For example, we can easily see that the structure of the conformal infinities in the regions I and III are identical to that of Minkowski space. We therefore call the Schwarzschild spacetime asymptotically flat. As in the Kruskal diagram, light cones stand upright and at  $45^\circ$  everywhere in the Conformal diagram.

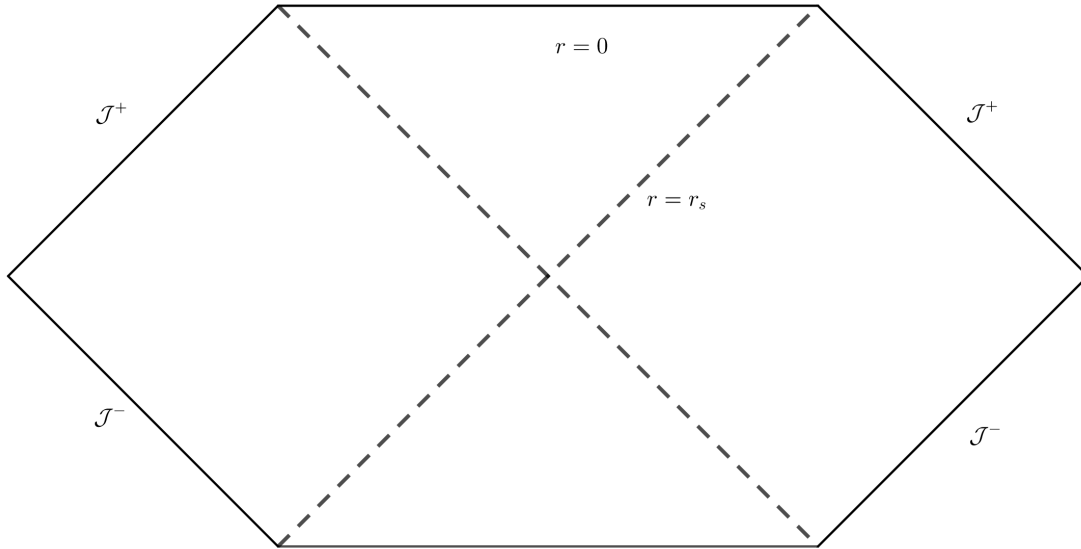


Figure 2: Conformal diagram for the maximally extended Schwarzschild spacetime. The future and past event horizons are located at  $r = r_s$ , while the curvature singularity is located at  $r = 0$ . Past null infinity  $\mathcal{J}^-$  is completely disjoint from future null infinity  $\mathcal{J}^+$  in the two asymptotically flat regions.

### 1.1.2 No-hair Theorem and the Information Paradox

Sean Carroll formulates a no-hair theorem in his book *Spacetime and Geometry* in the following way:

**Theorem 1.1. Black holes have no hair:** Stationary, asymptotically flat black hole solutions to general relativity coupled to electromagnetism, in 4 or less dimensions, that are nonsingular outside the event horizon, are fully characterized by the parameters of mass, electric and magnetic charge, and angular momentum. [1]

The essence of this theorem and the reason for its name, is that there are only a small number of properties, parameterizing all black hole solutions. Namely, the mass, charge and spin of the spacetimes. These quantities can be defined using for example the **Komar integrals**. This, together with phenomenon of **Hawking radiation** gives rise to the information paradox, that the information contained in matter seems to be lost when it passes the event horizon of a black hole.

### 1.1.3 The Kerr Black Hole

The Schwarzschild Black Hole already discussed is a lot less hairy than what is required by the above no-hair theorem; both its spin and its charge is zero. An example of a Black Hole solution with a non-zero spin would be the **Kerr Black Hole**, which has a quite intricate metric given in [1], which we will state in **Boyer-Lindquist coordinates** for completion:

$$ds^2 = - \left( 1 - \frac{2 G M r}{\rho^2} \right) dt^2 - \frac{2 G M a r \sin^2 \theta}{\rho^2} (dt d\phi + d\phi dt) + \frac{\rho^2}{\Delta} dr^2 + \rho^2 d\theta^2 + \frac{\sin^2 \theta}{\rho^2} [(r^2 + a^2)^2 - a^2 \Delta \sin^2 \theta] d\phi^2 \quad (1.4)$$

$$t \in (-\infty, \infty) \quad , \quad r \in (0, r_-) \cup (r_-, r_+) \cup (r_+, \infty) \quad , \quad \theta \in (0, \pi) \quad , \quad \phi \in (0, 2\pi) \quad (1.5)$$

The quantities  $\Delta$  and  $\rho$  are defined in terms of the coordinates and parameters as follow:

$$\Delta(r) = r^2 - 2 G M r + a^2 \quad (1.6)$$

$$\rho^2(r, \theta) = r^2 + a^2 \cos^2 \theta \quad (1.7)$$

The **Komar mass** and **Komar angular momentum** of the Kerr black hole are respectively  $M$  and  $Ma$ . The spacetime possesses a curvature singularity at  $\rho = 0$ , corresponding to  $r = 0$  and  $\theta = \frac{\pi}{2}$ . Unlike for the Schwarzschild black hole, the singularity is actually a ring and not a point. For this reason, it is referred to as a **ringularity**. The spacetime has two event horizons, an outer and an inner horizon, corresponding to the two values of  $r$  for which  $g^{rr} = 0$ :

$$g^{rr}(r) = 0 \quad \Rightarrow \quad r_{\pm} = G M \pm \sqrt{G^2 M^2 - a^2} \quad (1.8)$$

We will later explain this method of identifying event horizons in more detail, when we identify the horizons of the BTZ spacetime. In-between the inner and outer horizon, any future directed time-like curve is forced to move in the direction of decreasing  $r$ . In the region past the inner horizon, any time-like path is free to either go back through the inner horizon or go through the ringularity. The region past the ringularity is the extension of the spacetime to values of  $r < 0$ . It is sometimes referred to as the **anti universe**. It can easily be shown that the metric (1.4) restricted to curves of  $t = \text{const}$ ,  $r = \text{const}$  and  $\theta = \frac{\pi}{2}$ , with  $r \ll 1$ , becomes:

$$ds^2 \approx a^2 \left( 1 + \frac{2GM}{r} \right) d\phi^2 \quad (1.9)$$

Since  $\phi \sim \phi + 2\pi$ , it is clear that for  $r < 0$ , the curves described above become **closed time-like curves**. If instead of going through the ringularity, a time-like curve goes back through the inner horizon, it will be forced to move in the direction of decreasing  $r$  until it passes the outer horizon. Furthermore, it will not return to the asymptotically flat region it came from, but rather to a new asymptotically flat region. This all becomes more clear when looking at the Conformal diagram for the maximally extended Kerr spacetime:

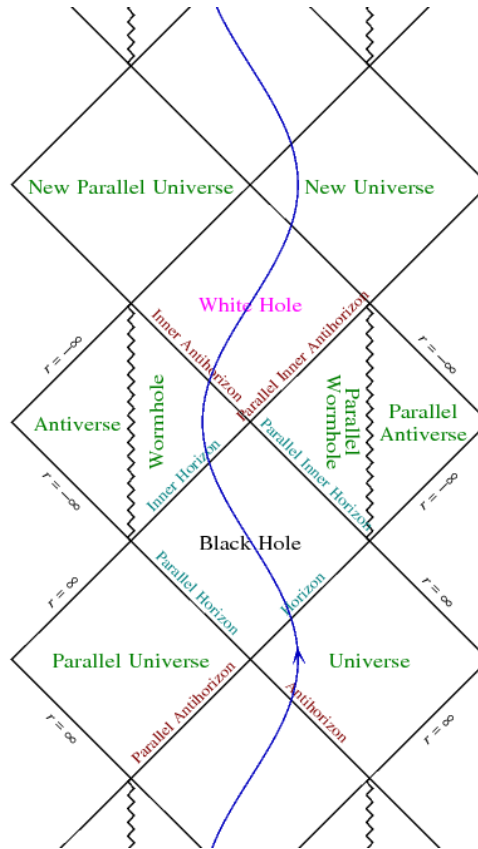


Figure 3: Conformal diagram for the Kerr spacetime. The blue line is the world line of a particle going through the wormhole. Found at <https://jila.colorado.edu/~ajsh/insidebh/penrose.html>



## 1.2 Aspects of QFT on curved backgrounds

In general curved spacetimes, there exist no notion of **global inertial coordinates**. As a consequence, there exists no preferred family of spacetime-foliations on which we can define a natural set of basis modes. Different sets of modes will be equally good and although they will exist in the same Hilbert space, they will define different Fock spaces, and specifically different vacuum states. A transformation between two sets of modes  $f_i$  and  $g_i$  is called a **Bogoliubov transformation** and given by [1]

$$g_i = \sum_j (\alpha_{ij} f_j + \beta_{ij} f_j^*) \quad , \quad f_i = \sum_j (\alpha_{ji}^* g_j - \beta_{ji} g_j^*) \quad (1.10)$$

The coefficients  $\alpha_{i,j}$  and  $\beta_{i,j}$  are called the Bogoliubov coefficients and also relate the annihilation and creation operators  $\hat{b}_i, \hat{b}_i^\dagger$  for  $g_i$  and  $\hat{a}_i, \hat{a}_i^\dagger$  for  $f_i$ .

$$\hat{a}_i = \sum_j (\alpha_{ji} \hat{b}_j + \beta_{ji}^* \hat{b}_j^\dagger) \quad , \quad \hat{b}_i = \sum_j (\alpha_{ij}^* \hat{a}_j - \beta_{ij} \hat{a}_j^\dagger) \quad (1.11)$$

We use this to calculate the expectation value of the number operator for  $g$ ,  $\hat{n}_{gi} = \hat{b}_i^\dagger \hat{b}_i$  in the vacuum state of  $f$ ,  $|0_f\rangle$ .

$$\langle 0_f | \hat{n}_{gi} | 0_f \rangle = \sum_j \beta_{ij} \beta_{ij}^* \quad (1.12)$$

And it now becomes apparent that what is a vacuum state for  $f$  is observed in  $g$  as a state containing particles.

### 1.2.1 The Unruh Effect

We will now briefly go through the simplest example of this difference in vacuum states, known as the Unruh effect, roughly following the structure of [1]. The Unruh effect can be stated as *"an accelerating observer in the traditional Minkowski vacuum state will observe a thermal spectrum of particles"* [1]

We start with ordinary (1+1)-dimensional Minkowski space and make the transformation

$$x = \frac{1}{a} e^{a\xi} \sinh(a\eta) \quad , \quad t = \frac{1}{a} e^{a\xi} \cosh(a\eta) \quad (1.13)$$

We call the coordinates  $(\xi, \eta)$  the **Rindler coordinates**. It can be shown that they cover the patch I given by  $x > |t|$  known as **Rindler space** and that we can cover the patch IV given by  $x < -|t|$  by simply adding a minus sign on each coordinate. In Rindler coordinates, curves of constant acceleration are given by

$$\eta(\tau) = \frac{\alpha}{a} \tau \quad , \quad \xi(\tau) = \frac{1}{a} \ln \left( \frac{a}{\alpha} \right) \quad (1.14)$$

and the metric takes the form

$$ds^2 = e^{2a\xi} (-d\eta^2 + d\xi^2) \quad (1.15)$$

Solving the Klein-Gordon equation  $\square \phi = 0$  in Rindler coordinates gives us plane waves, but because the future directed Killing vector is  $\partial_\eta$  and  $-\partial_\eta$  in patch I and IV respectively, we have a difference in sign for the positive frequency plane wave in the two regions, leading us to define two different plane wave solutions:

$$g_k^{(1)} = \begin{cases} \frac{1}{\sqrt{4\pi\omega}} e^{-i\omega\eta + ik\xi} & \text{I} \\ 0 & \text{IV} \end{cases} \quad (1.16)$$

$$g_k^{(2)} = \begin{cases} 0 & \text{I} \\ \frac{1}{\sqrt{4\pi\omega}} e^{i\omega\eta + ik\xi} & \text{IV} \end{cases} \quad (1.17)$$

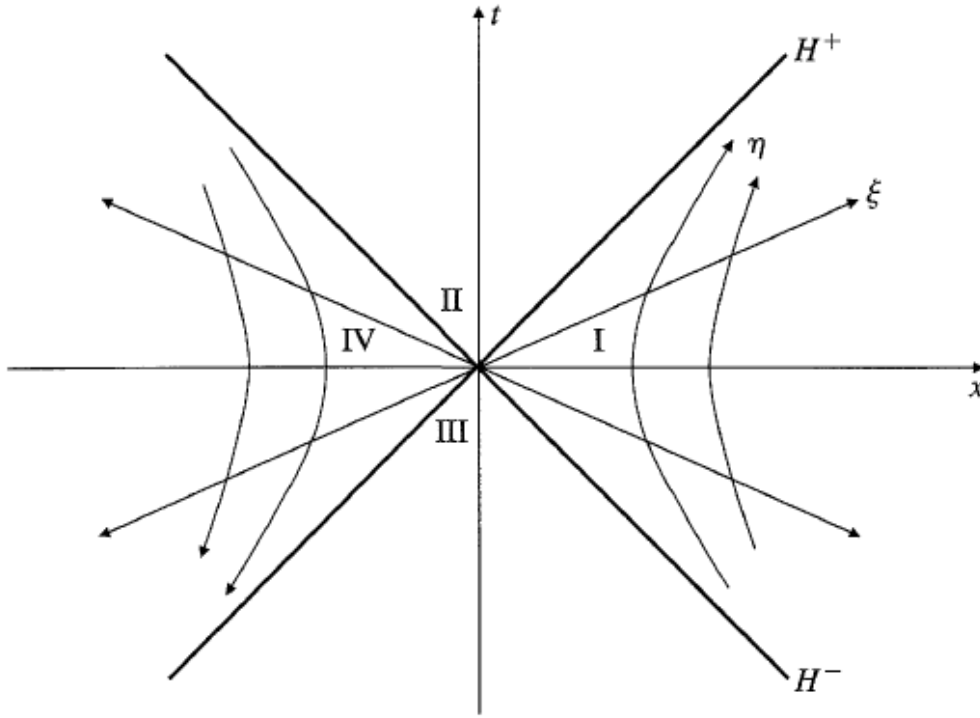


Figure 4: A picture of flat space in Rindler coordinates.  $H^+$  and  $H^-$  are killing horizons of  $\partial_\eta$ . Found in [1]

We now have two different but equally good sets of modes in Rindler and Minkowski coordinates. We could in theory calculate the Bogoliubov coefficients for these modes and use that to evaluate the expectation value of the number operator for the Rindler coordinates in the Minkowski vacuum. However such a calculation would be long and cumbersome. In [1] this calculation has been made easier by introducing a set of modes that share the vacuum state with Minkowski but is simpler connected to the Rindler modes. We will not go through his calculation, but state his result:

$$\langle 0_M | \hat{n}_R^{(1)}(k) | 0_M \rangle = \frac{1}{e^{2\omega\pi/a} - 1} \delta(0) \quad (1.18)$$

which is a thermal spectrum at the temp  $T = \frac{a}{2\pi}$ . This is exactly the Unruh effect. A static observer at the event horizon of a Schwarzschild black hole will feel the gravitational pull of the black hole and therefore must be accelerated in order to stay at constant  $r$ . This leads [1] to explain Hawking Radiation in terms of the Unruh effect by noting that the spacetime is locally flat at the event horizon. This argument seems to hold for objects much less exotic than black holes though, since any static observer close to a gravitational body must accelerate to remain at a fixed distance to that body. A more convincing way to show that we can associate a temperature with the black hole is to show that its **Green's Function** has all the properties of a thermal Green's Function. We will show this explicitly in (2+1) dimensions, where Einstein gravity has some special properties.

### 1.3 Gravity in (2+1) dimensions

One very important feature of standard Einstein gravity in (2+1) dimensions, is the fact that vacuum solutions have no local degrees of freedom. Said another way, all vacuum solutions to the **Einstein Equations** in (2+1) dimensions are locally isomorphic to one of the three maximally symmetric spaces; de Sitter space, ant-de Sitter space or Minkowski space. We will now show that this is indeed the case. Using the traces of the **Riemann tensor**; the **Ricci tensor** and **Ricci scalar**, we define a new

tensor  $C_{\rho\sigma\mu\nu}$ , called the **Weyl tensor**. This tensor is defined by:

$$C_{\rho\sigma\mu\nu} = R_{\rho\sigma\mu\nu} - \frac{2}{(n-2)} (g_{\rho[\mu} R_{\nu]\sigma} - g_{\sigma[\mu} R_{\nu]\rho}) + \frac{2}{(n-1)(n-2)} g_{\rho[\mu} g_{\nu]\sigma} R \quad (1.19)$$

The Weyl tensor possesses the same symmetries as the Riemann tensor, and satisfies the condition:

$$C^\rho{}_{\sigma\rho\nu} = 0 \quad (1.20)$$

Because the Weyl tensor and the Riemann tensor have the same symmetries, the LHS of (1.20) will be a symmetric tensor. It can be shown that the number of independent components of the Riemann tensor  $D_{Riem}$ , on an  $n$ -dimensional manifold is given by:

$$D_{Riem} = \frac{n^2(n^2-1)}{12} \quad (1.21)$$

The number of independent components of a symmetric  $(0,2)$ -tensor  $D_{sym}$ , on an  $n$ -dimensional manifold is of course given by:

$$D_{sym} = \frac{n(n+1)}{2} \quad (1.22)$$

Thus, the number of independent components of the Weyl tensor  $D_{Weyl}$ , on an  $n$ -dimensional manifold will be given by:

$$D_{Weyl} = D_{Riem} - D_{sym} = \frac{n^2(n^2-1)}{12} - \frac{n(n+1)}{2} \quad (1.23)$$

We see that for  $n = 3$ , we have  $D_{Weyl} = 0$ . Thus, in a 3-dimensional spacetime, we can use (1.19) to express the Riemann tensor in terms of its traces:

$$R_{\rho\sigma\mu\nu} = 2(g_{\rho[\mu} R_{\nu]\sigma} - g_{\sigma[\mu} R_{\nu]\rho}) - g_{\rho[\mu} g_{\nu]\sigma} R \quad (1.24)$$

Now we look at the **Einstein Equations** in vacuum with a cosmological constant  $\Lambda$ :

$$R_{\mu\nu} - \frac{1}{2} R g_{\mu\nu} + \Lambda g_{\mu\nu} = 0 \quad (1.25)$$

Taking the trace of (1.25) we obtain, on a 3-dimensional spacetime, the relation:

$$R = 6\Lambda \quad (1.26)$$

If we now substitute (1.26) back into (1.25), we obtain the equation:

$$R_{\mu\nu} = 2\Lambda g_{\mu\nu} \quad (1.27)$$

Thus, for a metric on a 3-dimensional spacetime, satisfying (1.25), the Riemann tensor takes the form:

$$\boxed{R_{\rho\sigma\mu\nu} = \Lambda (g_{\rho\mu} g_{\nu\sigma} - g_{\rho\nu} g_{\mu\sigma})} \quad (1.28)$$

We now see that any solution to the Einstein equations, on a 3-dimensional spacetime, will locally be isomorphic to a **maximally symmetric** space ( $dS_3$ ,  $AdS_3$  or  $M_3$ , depending on the sign of  $\Lambda$ ).

## 2 Derivation of the BTZ metric

As we proved in the last section, all vacuum solutions to the **Einstein Equations** in (2+1) dimensions are locally isomorphic to either de Sitter space, anti-de Sitter space or Minkowski space. Thus, all the information about any particular solution will be contained in its topology. Despite this, it is still very worthwhile to derive the BTZ metric in what we will call **Schwarzschild-like coordinates**, under the assumptions of stationarity and circular symmetry. There are several reasons for this, some of which being: it is easy to identify event horizons, the mass and angular momentum parameters will stand out clearly and the description of the spacetime in terms of identifying points in  $AdS_3$  will be particularly simple. With all that said, let us begin the derivation.

### 2.1 An ansatz for the Einstein Equations

On a 3-dimensional spacetime, a general metric tensor will have  $3(3+1)/2 = 6$  independent components, 3 of which can be arbitrarily changed by coordinate transformations. We will use this freedom to assume the following form of the metric:

$$ds^2 = -f^2(t, r, \phi) dt^2 + g^2(t, r, \phi) dr^2 + r^2 [d\phi - h(t, r, \phi) dt]^2 \quad (2.1)$$

We will discuss the ranges of these coordinates when the metric is fully derived. We assume of (2.1) that it be both stationary and circularly symmetric. This corresponds to the metric possessing two **Killing vectors**:  $R = \partial_\phi$ ,  $K = \partial_t$ . In order for (2.1) to be invariant under the flow of  $R$  and  $K$ , the metric must satisfy the conditions:

$$\begin{aligned} \mathcal{L}_R g_{\mu\nu} &= R^\lambda \frac{\partial g_{\mu\nu}}{\partial x^\lambda} + g_{\lambda\nu} \frac{\partial R^\lambda}{\partial x^\mu} + g_{\mu\lambda} \frac{\partial R^\lambda}{\partial x^\nu} = \frac{\partial g_{\mu\nu}}{\partial \phi} = 0 \\ \mathcal{L}_K g_{\mu\nu} &= K^\lambda \frac{\partial g_{\mu\nu}}{\partial x^\lambda} + g_{\lambda\nu} \frac{\partial K^\lambda}{\partial x^\mu} + g_{\mu\lambda} \frac{\partial K^\lambda}{\partial x^\nu} = \frac{\partial g_{\mu\nu}}{\partial t} = 0 \end{aligned} \quad (2.2)$$

Where  $\mathcal{L}_X$  is the **Lie derivative** in the direction of the vector  $X$ . The conditions (2.2) simply implies that the components of the metric be independent of  $\phi$  and  $t$ . We can thus write the metric (2.1), our ansatz for the Einstein Equations, in the form:

$$ds^2 = -f^2(r) dt^2 + g^2(r) dr^2 + r^2 [d\phi - h(r) dt]^2 \quad (2.3)$$

### 2.2 Solving the Einstein Equations

In section 1.3 on Einstein gravity in (2+1) dimensions, we found that the vacuum **Einstein equations** on a 3-dimensional spacetime, could be brought to the following form:

$$R_{ij} = 2\Lambda g_{ij} \quad (2.4)$$

In order to find solutions to (2.4), we first compute the **Ricci tensor**  $R_{ij}$ . We will do this using the **orthonormal frame method**, also sometimes called the triad method. We start by constructing an orthonormal basis of 1-forms  $\epsilon^i$ :

$$\epsilon^0 = f(r) dt, \quad \epsilon^1 = g(r) dr, \quad \epsilon^2 = r [d\phi - h(r) dt] \quad (2.5)$$

In the basis of the orthonormal 1-forms  $\epsilon^i$ , the metric manifestly becomes diagonal, meaning that:

$$ds^2 = \eta_{ij} \epsilon^i \otimes \epsilon^j = -\epsilon^0 \otimes \epsilon^0 + \epsilon^1 \otimes \epsilon^1 + \epsilon^2 \otimes \epsilon^2 \quad (2.6)$$

We can now employ the orthonormal 1-form basis  $\epsilon^i$  to find the **connection 1-forms**  $\omega^i_j$ , using the first **Cartan structure equation**:

$$\Theta^i = d\epsilon^i + \omega^i_j \wedge \epsilon^j = 0 \quad (2.7)$$

The components  $g_{ij}$  are the metric components with respect to the basis  $\epsilon^i$ , and  $\Theta^i$  are the **torsion 2-forms**. The requirement that our connect be torsion-free and metric compatible, impose the following requirements on  $\Theta^i$  and  $\omega^i_j$ :

$$\Theta^i = 0 \quad , \quad \omega_{ij} = -\omega_{ji} \quad , \quad \omega_{ij} := g_{ik} \omega^k_j \quad (2.8)$$

We now look for solutions to (2.7) satisfying the requirements (2.8). We start by computing the exterior derivative of our basis 1-forms  $\epsilon^i$ :

$$d\epsilon^0 = F(r) \epsilon^1 \wedge \epsilon^0 \quad , \quad d\epsilon^1 = 0 \quad , \quad d\epsilon^2 = G(r) \epsilon^1 \wedge \epsilon^2 - H(r) \epsilon^1 \wedge \epsilon^0 \quad (2.9)$$

Here, the functions  $F(r)$ ,  $G(r)$  and  $H(r)$ , are given in terms of  $f(r)$ ,  $g(r)$  and  $h(r)$  by:

$$F(r) := \frac{f'(r)}{f(r)g(r)} \quad , \quad G(r) := \frac{1}{r g(r)} \quad , \quad H(r) := \frac{r h'(r)}{f(r)g(r)} \quad (2.10)$$

The structure equation (2.7) with restrictions (2.8) in our orthonormal basis  $\epsilon^i$  then becomes:

$$\begin{aligned} F(r) \epsilon^1 \wedge \epsilon^0 + \omega^0_1 \wedge \epsilon^1 + \omega^0_2 \wedge \epsilon^2 &= 0 \\ \omega^1_0 \wedge \epsilon^0 + \omega^1_2 \wedge \epsilon^2 &= 0 \\ G(r) \epsilon^1 \wedge \epsilon^2 - H(r) \epsilon^1 \wedge \epsilon^0 + \omega^2_0 \wedge \epsilon^0 + \omega^2_1 \wedge \epsilon^1 &= 0 \end{aligned} \quad (2.11)$$

Upon inspection, one finds that the following is a set of solutions to the above equations:

$$\omega^0_1 = F(r) \epsilon^0 - \frac{1}{2} H(r) \epsilon^2 \quad , \quad \omega^2_1 = G(r) \epsilon^2 - \frac{1}{2} H(r) \epsilon^0 \quad , \quad \omega^2_0 = \frac{1}{2} H(r) \epsilon^1 \quad (2.12)$$

We can now use the second **Cartan structure equation** to compute the **curvature 2-forms**:

$$\Omega^i_j = d\omega^i_j + \omega^i_k \wedge \omega^k_j \quad (2.13)$$

We begin by computing the exterior derivative of each connection 1-form. The result is the following:

$$\begin{aligned} d\omega^0_1 &= \left[ \frac{F'(r)}{g(r)} + F^2(r) - \frac{H^2(r)}{2} \right] \epsilon^1 \wedge \epsilon^0 + \left[ \frac{H'(r)}{2g(r)} + \frac{H(r)G(r)}{2} \right] \epsilon^1 \wedge \epsilon^2 \\ d\omega^2_1 &= \left[ \frac{G'(r)}{g(r)} + G^2(r) \right] \epsilon^1 \wedge \epsilon^2 - \left[ G(r)H(r) + \frac{H'(r)}{2g(r)} + \frac{H(r)F(r)}{2} \right] \epsilon^1 \wedge \epsilon^0 \\ d\omega^2_0 &= 0 \end{aligned} \quad (2.14)$$

We now compute the wedge products between the connection 1-forms. The result is the following:

$$\begin{aligned} \omega^0_2 \wedge \omega^2_1 &= \frac{H(r)G(r)}{2} \epsilon^1 \wedge \epsilon^2 - \frac{H^2(r)}{4} \epsilon^1 \wedge \epsilon^0 \\ \omega^2_0 \wedge \omega^0_1 &= \frac{H(r)F(r)}{2} \epsilon^1 \wedge \epsilon^0 + \frac{H^2(r)}{4} \epsilon^1 \wedge \epsilon^2 \\ \omega^2_1 \wedge \omega^1_0 &= - \left[ G(r)F(r) + \frac{H^2(r)}{4} \right] \epsilon^0 \wedge \epsilon^2 \end{aligned} \quad (2.15)$$

Using the results (2.15) and (2.16), we see that the second Cartan structure equation (2.13) reads:

$$\begin{aligned}\Omega^0_1 &= \left[ \frac{F'(r)}{g(r)} + F^2(r) - \frac{3H^2(r)}{4} \right] \epsilon^1 \wedge \epsilon^0 + \left[ \frac{H'(r)}{2g(r)} + H(r)G(r) \right] \epsilon^1 \wedge \epsilon^2 \\ \Omega^2_1 &= \left[ \frac{G'(r)}{g(r)} + G^2(r) + \frac{H^2(r)}{4} \right] \epsilon^1 \wedge \epsilon^2 - \left[ G(r)H(r) + \frac{H'(r)}{2g(r)} \right] \epsilon^1 \wedge \epsilon^0 \\ \Omega^2_0 &= - \left[ G(r)F(r) + \frac{H^2(r)}{4} \right] \epsilon^0 \wedge \epsilon^2\end{aligned}\quad (2.16)$$

The curvature 2-forms are related to the **Riemann tensor** components  $R^i_{jkl}$ , in the following way:

$$\Omega^i_j = \frac{1}{2} R^i_{jkl} \epsilon^k \wedge \epsilon^l \quad (2.17)$$

The non-zero components (*excluding those related by symmetry*) of the Riemann tensor are thus:

$$\begin{aligned}R^0_{110} &= \frac{F'(r)}{g(r)} + F^2(r) - \frac{3H^2(r)}{4} \\ R^0_{112} &= \frac{H'(r)}{2g(r)} + H(r)G(r) \\ R^2_{112} &= \frac{G'(r)}{g(r)} + G^2(r) + \frac{H^2(r)}{4} \\ R^2_{002} &= -G(r)F(r) - \frac{H^2(r)}{4}\end{aligned}\quad (2.18)$$

From the above components of the Riemann tensor, we can now construct the non-zero components (*excluding those related by symmetry*) of the **Ricci tensor**  $R_{jl} := R^i_{jil}$ . The result is the following:

$$\begin{aligned}R_{00} &= \frac{F'(r)}{g(r)} + F^2(r) - \frac{H^2(r)}{2} + G(r)F(r) \\ R_{02} &= \frac{H'(r)}{g(r)} + 2H(r)G(r) \\ R_{11} &= -\frac{F'(r)}{g(r)} - F^2(r) + \frac{H^2(r)}{2} - \frac{G'(r)}{g(r)} - G^2(r) \\ R_{22} &= -\frac{G'(r)}{g(r)} - G^2(r) - \frac{H^2(r)}{2} - G(r)F(r)\end{aligned}\quad (2.19)$$

We are now ready to solve the vacuum Einstein Equations (2.4). The 02-component of the Einstein Equations immediately let us solve for the function  $H(r)$ :

$$R_{02} = 0 \quad \Rightarrow \quad r H'(r) + 2 H(r) = 0 \quad \Rightarrow \quad H(r) = -\frac{J}{r^2} \quad (2.20)$$

Where  $J \in \mathbb{R}$ . As the name suggests, the integration constant  $J$  is indeed the angular momentum of the spacetime. A discussion of this can be found in [3]. In order to find the function  $G(r)$ , it is convenient to consider the following sum of Ricci components:

$$2\Lambda = R_{00} + R_{11} + R_{22} = -2r G'(r)G(r) - 2G^2(r) - \frac{H^2(r)}{2} \quad (2.21)$$

If we now define a new function:  $\Gamma(r) = r G(r)$ , we get the following first order equation for  $\Gamma(r)$ :

$$2\Gamma'(r)\Gamma(r) + \frac{r H^2(r)}{2} = -2r\Lambda \quad \Rightarrow \quad \Gamma^2(r) = -M - \Lambda r^2 + \frac{J^2}{4r^2} \quad (2.22)$$

Where  $M \in \mathbb{R}$ . Again, as the name suggests, the integration constant  $M$  turns out to be the mass of the spacetime. As with  $J$ , a discussion of this can be found in [3]. If we compare the above result with the relations (2.10), we see that:

$$g^{-2}(r) = r^2 G^2(r) = \Gamma^2(r) \Rightarrow g^{-2}(r) = -M - \Lambda r^2 + \frac{J^2}{4r^2} \quad (2.23)$$

In order to find the function  $f(r)$ , it is convenient to consider the following sum of Ricci components:

$$0 = R_{00} + R_{11} = -G(r) \Gamma'(r) + G(r) F(r) \Rightarrow \frac{F(r)}{\Gamma(r)} = \frac{\Gamma'(r)}{\Gamma(r)} \quad (2.24)$$

From the above equation (2.10) and (2.24), we find the following relation between  $f(r)$  and  $g(r)$ :

$$\frac{F(r)}{\Gamma(r)} = \frac{f'(r)}{f(r)} \Rightarrow \frac{\Gamma'(r)}{\Gamma(r)} = \frac{f'(r)}{f(r)} \Rightarrow k^2 g^{-2}(r) = f^2(r) \quad (2.25)$$

Where  $k \in \mathbb{R}$ . Lastly, we get from (2.10) and (2.25) the following first order equation for  $h(r)$ :

$$h'(r) = \frac{k H(r)}{r} = -\frac{k J}{r^3} \Rightarrow h(r) = \frac{k J}{2 r^2} + c \quad (2.26)$$

Where  $c \in \mathbb{R}$ . The integration constants  $k$  and  $c$  can be removed from the solution, by performing the following simple coordinate transformation:

$$\phi \rightarrow \phi - c t, \quad t \rightarrow k t \quad (2.27)$$

Thus, the final form of the metric (2.3) becomes:

$$ds^2 = - \left[ -M - \Lambda r^2 + \frac{J^2}{4r^2} \right] dt^2 + \left[ -M - \Lambda r^2 + \frac{J^2}{4r^2} \right]^{-1} dr^2 + r^2 \left[ d\phi - \frac{J}{2r^2} dt \right]^2 \quad (2.28)$$

When  $\Lambda < 0$ , this metric behaves like a black hole metric, and is called the **BTZ black hole** metric. To see that  $\Lambda < 0$  is necessary for (2.28) to be a black hole, one option is to investigate how the causal type (*time-like, space-like or null*) of constant  $r$  hypersurfaces changes with  $r$ . For black holes, we expect to see at least one value of  $r$  for which the associated hypersurface is null, and we expect the hypersurfaces to be time-like for  $r \rightarrow \infty$ . In the coordinates  $(t, r, \phi)$ , the normal vectors of constant  $r$  hypersurfaces  $n^\mu = g^{\mu\nu} (\partial_\nu r)$ , have the following metric norms:

$$g_{\mu\nu} n^\mu n^\mu = g_{\mu\nu} g^{\mu\rho} (\partial_\rho r) g^{\nu\sigma} (\partial_\sigma r) = g^{rr}(r) \quad (2.29)$$

Thus, the values of  $r^2$  for which the constant  $r$  hypersurfaces become null are the following:

$$\begin{aligned} \Lambda \neq 0 : \quad g^{rr}(r) = 0 &\Rightarrow r_\pm^2 = -\frac{1}{2\Lambda} [M \pm \sqrt{M^2 + \Lambda J^2}] \\ \Lambda = 0 : \quad g^{rr}(r) = 0 &\Rightarrow r_+^2 = \frac{J^2}{4M} \end{aligned} \quad (2.30)$$

The number of solutions to the above equations depend on the sign of the cosmological constant  $\Lambda$ , and so does the sign of  $g^{rr}(r)$  as  $r$  varies, which determines the causal type of the hypersurfaces:

$\Lambda > 0$ : there will be 0 or 1 solutions to (2.30) with  $r^2 > 0$ , and  $g^{rr}(r) < 0$  as  $r \rightarrow \infty$ .

$\Lambda = 0$ : there will be 0 or 1 solutions to (2.30) with  $r^2 > 0$ , and  $g^{rr}(r) < 0$  as  $r \rightarrow \infty$ .

$\Lambda < 0$ : there will be 0, 1 or 2 solutions to (2.30) with  $r^2 > 0$ , and  $g^{rr}(r) > 0$  as  $r \rightarrow \infty$ .

The crucial point here, is that only for  $\Lambda < 0$ , constant  $r$  hypersurfaces will be time-like at infinity. Thus, the BTZ spacetime will have the causal structure of a black hole only when  $\Lambda < 0$ . In the non-degenerate case, the spacetime will possess an outer and an inner event horizon, just as the (3+1) dimensional **Kerr black hole**. Thus, the ranges of the coordinates  $(t, r, \phi)$  are:

$$t \in (-\infty, \infty) \quad , \quad r \in (0, r_-) \cup (r_-, r_+) \cup (r_+, \infty) \quad , \quad \phi \in (0, 2\pi) \quad (2.31)$$

The BTZ black hole has many other properties similar to those of black hole solutions in (3+1) dimensions, in particular the Kerr black hole. We will further explore these similarities, and important differences, in section 3.

## 2.3 Connection to anti-de Sitter space

Now that we have established that the BTZ metric only describes a black hole spacetime when  $\Lambda < 0$ , we can begin to investigate how this affects the structure of the BTZ spacetime. From our discussion of Einstein gravity in (2+1) (*section 1.3*) we know that  $\Lambda < 0$  implies that the BTZ spacetime be locally isomorphic to 3 dimensional anti-de Sitter space,  $AdS_3$ . This means that we can potentially learn a lot about the BTZ spacetime by studying  $AdS_3$ , and we will now proceed to do so.

### 2.3.1 Anti-de Sitter space

One way of defining  $AdS_3$  is by introducing an ambient  $\mathbb{R}^4$  space, equipped with the following metric:

$$dS^2 = \eta_{ab}^{(2,2)} dX^a dX^b = -(dX^0)^2 - (dX^1)^2 + (dX^2)^2 + (dX^3)^2 \quad (2.32)$$

$AdS_3$  is then defined as a hypersurface in the ambient  $\mathbb{R}^4$  space, through the following constraint:

$$\eta_{ab}^{(2,2)} X^a X^b = -(X^0)^2 - (X^1)^2 + (X^2)^2 + (X^3)^2 = -\ell^2 \quad (2.33)$$

We can now parametrize the points in  $\mathbb{R}^4$  satisfying (2.33), with the coordinates  $(\lambda, \rho, \theta)$  as follow:

$$\begin{aligned} X^0 &= \ell \sin \lambda \cosh \rho \quad , \quad X^1 = \ell \cos \lambda \cosh \rho \\ X^2 &= \ell \sin \theta \sinh \rho \quad , \quad X^3 = \ell \cos \theta \sinh \rho \\ \lambda &\in (-\infty, \infty) \quad , \quad \rho \in (0, \infty) \quad , \quad \theta \in (0, 2\pi) \end{aligned} \quad (2.34)$$

The **pull-back** of the ambient metric (2.32) onto the  $AdS_3$  hypersurface (2.33), is then given by:

$$ds^2 = g_{\mu\nu} dx^\mu dx^\nu = \ell^2 (-\cosh^2 \rho d\lambda^2 + d\rho^2 + \sinh^2 \rho d\theta^2) \quad (2.35)$$

It should be noted that because we have chosen for  $\lambda \in (-\infty, \infty)$ , what we have constructed is technically the universal covering space of  $AdS_3$ , sometimes denoted by  $\widetilde{AdS_3}$ . we have done this to avoid the emergence of **closed time-like curves**, normally associated with the construction of  $AdS_3$  as the hypersurface (2.33). The Ricci tensor  $R_{\mu\nu}$  and Ricci scalar  $R$  can now be computed from the metric (2.35). It can easily be checked that  $R_{\mu\nu} = -2\ell^{-2} g_{\mu\nu}$  and  $R = -6\ell^{-2}$ , confirming that  $AdS_3$  is the constant negative curvature solution to the vacuum Einstein Equations with  $\Lambda = -\ell^{-2}$ .

To investigate the causal structure of  $AdS_3$  it is, as always, useful to construct a conformal diagram of the spacetime. In order to so, we perform the following coordinate transformation of the radial coordinate  $\rho$ :

$$\cosh \rho = \frac{1}{\cos \chi} \quad \Rightarrow \quad ds^2 = \frac{\ell^2}{\cos^2 \chi} (-d\lambda^2 + d\chi^2 + \sin^2 \chi d\theta^2) \quad (2.36)$$

From the above relation between  $\rho$  and  $\chi$ , we can clearly see that  $\chi \in (0, \frac{\pi}{2})$ .  $AdS_3$  is therefore conformally equivalent to an infinite strip of width  $\frac{\pi}{2}$ , as can be seen in the conformal diagram below:



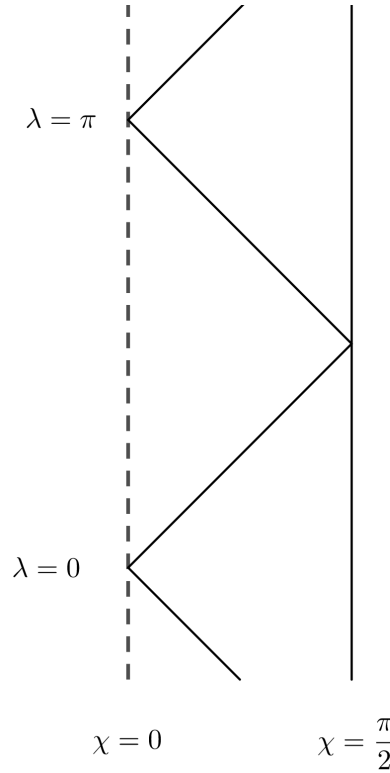


Figure 5: Conformal diagram of anti-de Sitter space. We see that light rays can emerge at conformal infinity  $\mathcal{I}$  at any  $\lambda$ , and subsequently terminate at  $\mathcal{I}$  at a later  $\lambda$ . Thus, there are no **Cauchy surfaces** in  $AdS_3$ , and consequently we do not have well-posed initial value problems on the  $AdS_3$  spacetime.

Looking at the above conformal digram, we see a very interesting causal property of  $AdS_3$ , namely that conformal infinity  $\mathcal{I}$  is a time-like hypersurface. As a consequence of this fact,  $AdS_3$  is not globally hyperbolic, meaning that it has no **Cauchy surfaces**. This is because there exists null geodesics which both emerge and terminate at  $\mathcal{I}$ . Thus, we do not have well-posed initial value problems on the  $AdS_3$  in terms of information specified on a Cauchy surface. Later in section 4.1, when we compute **Green's functions** on the BTZ spacetime, the fact that  $AdS_3$  is not globally hyperbolic will force us to choose boundary condition for the scalar field at infinity. More details will follow in said section.

### 2.3.2 Constructing the BTZ spacetime

As we have already mentioned previously, any solution to the vacuum Einstein Equatins in (2+1) must be locally isomorphic to  $AdS_3$ . Thus, the BTZ spacetime must also be locally isomorphic to  $AdS_3$ . However, there is no guarantee that the global structure of the BTZ spacetime should be related to that of  $AdS_3$  in any simple way. Fortunately, it turns out that the global structures of BTZ and  $AdS_3$  actually *is* related in a simple way. This is most easilly seen by covering the hypersurface (2.33) with a set of coordinates  $(t, r, \phi)$ , as defined in appendix B. It is easy to verify that the pull-back of the metric (2.32) onto the  $AdS_3$  hypersurface, using the coordinates  $(t, r, \phi)$ , recovers the BTZ metric (2.28) in each of the regions **I**, **II** and **III**, with  $\Lambda = -\ell^{-2}$ . In order for the  $(t, r, \phi)$  coordinates to cover all of  $AdS_3$ , they must have the following ranges:

$$r \in (0, r_-) \cup (r_-, r_+) \cup (r_+, \infty) \quad , \quad \phi \in (-\infty, \infty) \quad , \quad t \in (-\infty, \infty) \quad (2.37)$$

This is exactly the ranges of the Schwarzschild-like coordinates on the BTZ spacetime, except that  $\phi$  is here an uncompact coordinate. Thus, we arrive at the amazing fact that the BTZ spacetime can be constructed from  $AdS$ , by identifying points such that  $\phi \sim \phi + 2\pi$ . This fact will greatly aid us in section 4.1, when we set out to find Green's functions on the BTZ spacetime.

### 3 Classical properties of the BTZ spacetime

As mentioned back in section 2.2, the BTZ spacetime has many features in common with black hole solutions in (3+1) dimensions, and in particular the Kerr black hole. As was pointed out during the derivation of the BTZ metric in section 2.2, a mass  $M$  and angular momentum  $J$  can be defined for the spacetime. It also posses two event horizons at:

$$r_{\pm}^2 = \frac{\ell^2}{2} \left[ M \pm \sqrt{M^2 - \left(\frac{J}{\ell}\right)^2} \right] \quad (3.1)$$

As was also shown in section 2.2. Just like the Kerr black hole, the BTZ black hole also posses an **ergosphere**, which is a region between the outer horizon and the so-called **ergo shell**. In Schwarzschild-like coordinates, the ergo shell is defined as the hypersurafce on which  $\partial_t$  becomes null, and thus:

$$g_{tt}(r) = 0 \quad \Rightarrow \quad -M + \frac{r^2}{\ell^2} = 0 \quad \Rightarrow \quad r_{erg}^2 = M \ell^2 \geq r_+^2 \quad (3.2)$$

The interesting thing about the ergosphere is that time-like curves in this region must partially be moving in the direction of  $\partial_\phi$ , as the only negative metric component in this region is  $g_{t\phi}$ .

We have now exhausted the list of interesting properties of the BTZ spacetime which can easily be extracted from its mettric. To better be able to investigate the causal properties of the BTZ spacetime, we now proceed to derive its conformal digram.

#### 3.1 Causal structure of the spacetime

We will here focus on deriving a conformal digram for the case of  $J = 0$ ; the static BTZ black hole. The metric for the static BTZ black hole is given by:

$$ds^2 = -f^2(r) dt^2 + f^{-2}(r) dr^2 + r^2 d\phi^2 \quad , \quad f^2(r) = -M + \frac{r^2}{\ell^2} \quad (3.3)$$

$$-\infty < t < \infty, \quad 0 < r < \infty, \quad 0 \leq \phi < 2\pi$$

Because this metric is so similar to the (3+1)-dimensional Schwarzschild black hole, we can follow the usual derivation as seen in [1] of Kruskal coordinates and a Penrose diagram quite closely.

Before we start, we note that just like in the Schwarzschild metric, there appears to be a singularity at  $r = r_+ = \ell \sqrt{M}$ . As was the case with Schwarzschild, this is merely a coordinate singularity. Because it is shown in the exact same way as for Schwarzschild, we will not go through any trouble showing it explicitly, but it will be apparent once we see the conformal diagram. We start by introducing a so-called turtoise coordinate  $r^*$ , such that:

$$f^2(r) (dr^*)^2 = f^{-2}(r) dr^2 \quad \Rightarrow \quad \frac{dr^*}{dr} = f^{-2}(r) \quad (3.4)$$

$$\Rightarrow \quad r^*(r) = \int \frac{1}{\frac{r^2}{\ell^2} - M} dr = \frac{\ell^2}{2r_+} \int \frac{1}{r - r_+} - \frac{1}{r + r_+} dr = \frac{\ell^2}{2r_+} \ln \left( \frac{|r - r_+|}{r + r_+} \right) \quad (3.5)$$

We see that the  $r^*(r)$  is singular at  $r = r_+$ , so we only look at the case  $r > r_+$ , for which we do not need the absolute value. By changing to the turtoise coordinate, we can bring the metric to the form:

$$ds^2 = f^2(r) [-dt^2 + (dr^*)^2] + r^2(r^*) d\phi^2 \quad (3.6)$$

$$-\infty < t < \infty \quad , \quad -\infty < r^* < 0$$

It is now straightforward to define a pair of null coordinates  $v$  and  $u$ , using the above metric:

$$v = t + r^* \quad , \quad u = t - r^* \quad (3.7)$$

In terms of the new null coordinates  $v$  and  $u$ , the static BTZ metric now takes the following form:

$$ds^2 = -\frac{f^2(r)}{2} [du dv + dv du] + r^2 d\phi^2 \quad (3.8)$$

$$-\infty < u, v < \infty \quad , \quad v < u$$

We note that  $r$  is now to be interpreted as an implicit function of  $v$  and  $u$ , with the following relation:

$$\frac{1}{2}(v - u) = \frac{\ell^2}{2r_+} \ln \left( \frac{r - r_+}{r + r_+} \right) \quad (3.9)$$

Just like in the Schwarzschild case, the apparent coordinate singularity at  $r = r_+$  is moved to infinity in these coordinates. Fixing it requires us to write  $u$  and  $v$  in terms of our initial coordinates  $t$  and  $r$ :

$$v = t + r^* = t + \frac{\ell^2}{2r_+} \ln \left( \frac{r - r_+}{r + r_+} \right) \quad , \quad u = t - r^* = t - \frac{\ell^2}{2r_+} \ln \left( \frac{r - r_+}{r + r_+} \right) \quad (3.10)$$

We see now that a clever choice of coordinates  $v'$  and  $u'$ , might be given by the following:

$$v' = \exp \left( \frac{r+v}{\ell^2} \right) \quad , \quad u' = -\exp \left( \frac{-r+u}{\ell^2} \right) \quad (3.11)$$

These can be expressed in terms of the original coordinates  $t$  and  $r$ , in the following way:

$$v' = \sqrt{\frac{r - r_+}{r + r_+}} \exp \left( \frac{r+t}{\ell^2} \right) \quad , \quad u' = -\sqrt{\frac{r - r_+}{r + r_+}} \exp \left( \frac{-r+t}{\ell^2} \right) \quad (3.12)$$

In terms of the coordinates  $v'$  and  $u'$ , the static BTZ metric now takes the following form:

$$ds^2 = -\frac{f^2(r)}{2} \frac{\ell^4}{r_+^2} \left( \frac{r + r_+}{r - r_+} \right) [du' dv' + dv' du'] + r^2 d\phi^2 \quad (3.13)$$

$$0 < v' < \infty \quad , \quad -\infty < u' < 0 \quad , \quad v' u' < -1$$

We can simplify the above metric a bit by realizing that:

$$f^2(r) = -M + \frac{r^2}{\ell^2} = \frac{r^2 - r_+^2}{\ell^2} = \frac{(r - r_+)(r + r_+)}{\ell^2} = \frac{(r + r_+)^2}{\ell^2} \left( \frac{r - r_+}{r + r_+} \right) \quad (3.14)$$

Using the above expression for  $f^2(r)$ , we now find that:

$$ds^2 = -\frac{\ell^2}{2} \frac{(r + r_+)^2}{r_+^2} [du' dv' + dv' du'] + r^2 d\phi^2 \quad (3.15)$$

It is now apparent that  $r = r_+$  is not a real singularity, since the metric is not singular for this value of  $r$  in these coordinates. To get the Kruskal-like coordinates for the BTZ black holes, we just need to change back into a set of one time-like and two space-like coordinates, using the combination:

$$T = \frac{1}{2} (v' + u') \quad , \quad R = \frac{1}{2} (v' - u') \quad (3.16)$$

We can now write the coordinates  $T$  and  $R$ , in terms of the original coordinates  $t$  and  $r$ :

$$T = \frac{1}{2} \sqrt{\frac{r-r_+}{r+r_+}} \left[ \exp\left(\frac{r_+t}{\ell^2}\right) - \exp\left(\frac{-r_+t}{\ell^2}\right) \right] = \sqrt{\frac{r-r_+}{r+r_+}} \sinh\left(\frac{r_+t}{\ell^2}\right) \quad (3.17)$$

$$R = \frac{1}{2} \sqrt{\frac{r-r_+}{r+r_+}} \left[ \exp\left(\frac{r_+t}{\ell^2}\right) + \exp\left(\frac{-r_+t}{\ell^2}\right) \right] = \sqrt{\frac{r-r_+}{r+r_+}} \cosh\left(\frac{r_+t}{\ell^2}\right) \quad (3.18)$$

The metric for the static BTZ black hole, now takes a particularly simple form, in terms of  $T$  and  $R$ :

$$ds^2 = \ell^2 \frac{(r+r_+)^2}{r_+^2} [-dT^2 + dR^2] + r^2 d\phi^2 \quad (3.19)$$

$$-\infty < T, R < \infty, \quad -1 < R^2 - T^2 < 1, \quad 0 \leq \phi < 2\pi$$

It is easily seen from (3.18) and (3.16), that  $R^2 - T^2 > 0$  and  $R > 0$ , for  $r > r_+$ . But space-like geodesics can reach  $R = 0$  at finite parameter value, so there must be more spacetime beyond this. We can cover this other patch by a set of coordinates similar to (3.18) and (3.17), but with a minus sign on each coordinate (*so that  $R < 0$ ; we see that these two patches do not overlap*).

When we defined the tortoise coordinate  $r^*$ , we noted that it was singular at  $r = r_+$ , and chose to look at only  $r > r_+$ . Had we instead chosen  $0 < r < r_+$ , we would have simply swapped the order of  $r_+$  and  $r$  when we removed the absolute value, such that:

$$r^* = \frac{\ell^2}{2r_+} \ln\left(\frac{r_+ - r}{r + r_+}\right) \quad (3.20)$$

This would have given us a minus sign in (3.14), which would have lead to us swapping the definitions of  $T$  and  $R$  in (3.16), and consequently the definitions of  $T$  and  $R$  in terms of  $t$  and  $r$  would be swapped as well. This would correspond to a patch in which  $R^2 - T^2 < 0$  and  $T > 0$ . In this patch of spacetime, it is possible for time-like geodesics to reach  $T = 0$  at finite parameter value, so there must be more spacetime beyond this as well. We can, once again, cover this new patch by simply adding a minus sign to each coordinate  $T$  and  $R$ . This leaves us with the maximally extended spacetime for the static BTZ black hole, consisting of four patches with the following coordinates:

**I**  $(r_+ < r)$

$$T = \sqrt{\frac{r-r_+}{r+r_+}} \sinh\left(\frac{r_+t}{\ell^2}\right), \quad R = \sqrt{\frac{r-r_+}{r+r_+}} \cosh\left(\frac{r_+t}{\ell^2}\right) \quad (3.21)$$

**II**  $(0 < r < r_+)$

$$T = \sqrt{\frac{r_+-r}{r+r_+}} \cosh\left(\frac{r_+t}{\ell^2}\right), \quad R = \sqrt{\frac{r_+-r}{r+r_+}} \sinh\left(\frac{r_+t}{\ell^2}\right) \quad (3.22)$$

**III**  $(r_+ < r)$

$$T = -\sqrt{\frac{r-r_+}{r+r_+}} \sinh\left(\frac{r_+t}{\ell^2}\right), \quad R = -\sqrt{\frac{r-r_+}{r+r_+}} \cosh\left(\frac{r_+t}{\ell^2}\right) \quad (3.23)$$

**IV**  $(0 < r < r_+)$

$$T = -\sqrt{\frac{r_+-r}{r+r_+}} \cosh\left(\frac{r_+t}{\ell^2}\right), \quad R = -\sqrt{\frac{r_+-r}{r+r_+}} \sinh\left(\frac{r_+t}{\ell^2}\right) \quad (3.24)$$

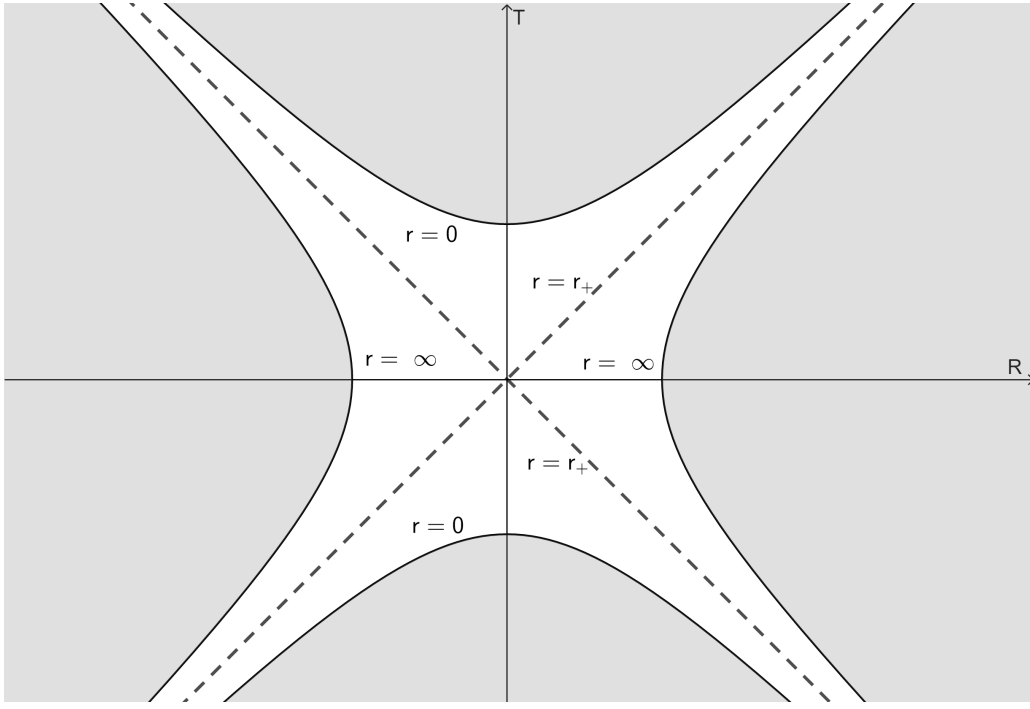


Figure 6: The Kruskal-diagram for the static BTZ black hole. Light rays move on  $45^\circ$  lines in these coordinates. The past and future event horizons are null surfaces located at  $r = r_+$ . The grey areas are not part of the spacetime.

Patch I and III corresponds to two different asymptotically  $AdS_3$  parts of the spacetime (*as will be clear when the conformal digram is constructed*), while II and IV are the black and white hole respectively. In patch I and III, we see that  $r = \text{const}$  corresponds to  $0 < R^2 - T^2 = \text{const} < 1$ , while  $t = \text{const}$  corresponds to  $-1 < T/R = \text{const} < 1$ . This means that constant  $r$  curves are hyperbolas while constant  $t$  curves are lines intersecting the origin, just as in the Schwarzschild case. The point at  $r = 0$  lies in patch II and IV, and are described by the hyperbolas:

$$R^2 - T^2 = -1 \quad (3.25)$$

Which is again just like the Schwarzschild case. Different from the Schwarzschild case however, is  $r = \infty$ , which usually lies at  $R^2 - T^2 = \infty$ , but now lies in patch I and III, and are described by:

$$R^2 - T^2 = 1 \quad (3.26)$$

If we want to construct a conformal diagram for the static BTZ spacetime, we can follow the approach of not only Schwarzschild but also flat space, and make another coordinate transformation:

$$v' = \tan(r_+ V) \quad , \quad u' = \tan(r_+ U) \quad (3.27)$$

$$\Rightarrow \quad dv' = \frac{r_+}{\cos^2(r_+ V)} dV \quad , \quad du' = \frac{r_+}{\cos^2(r_+ U)} dU \quad (3.28)$$

$$\Rightarrow \quad dv' du' + du' dv' = \frac{r_+^2}{\cos^2(\frac{V}{r_+}) \cos^2(\frac{U}{r_+})} [dV dU + dU dV] \quad (3.29)$$

We can now write the metric (3.15), using the coordinates  $V$  and  $U$ , in the follow way:

$$ds^2 = -\frac{\ell^2}{2} \frac{(r + r_+)^2}{\cos^2(r_+ V) \cos^2(r_+ U)} [dV dU + dU dV] + r^2 d\phi^2 \quad (3.30)$$

$$0 < V < \pi/2 \quad , \quad -\pi/2 < U < 0 \quad , \quad 0 \leq \phi < 2\pi$$

We now make one last transformation to one time-like and one space-like coordinate,  $T'$  and  $R'$ :

$$V = \frac{1}{2}(T' + R') \quad , \quad U = \frac{1}{2}(T' - R') \quad (3.31)$$

In terms of the time-like coordinate  $T'$  and space-like coordinate  $R'$ , the metric finally takes the form:

$$\begin{aligned} ds^2 &= \omega^{-2} [-(dT')^2 + (dR')^2] + r^2 d\phi^2 \\ \omega^{-2} &= \frac{2\ell^2 (r + r_+)^2}{[\cos(r_+ T') + \cos(r_+ R')]^2} \\ -\pi/2 &< T', R' < \pi/2 \quad , \quad 0 \leq \phi < 2\pi \end{aligned} \quad (3.32)$$

If we omit the angular part of the above metric, we now easily see that the rest of the metric is related by the conformal factor  $\omega^2$  to the metric of flat two dimensional Minkowski space:

$$\begin{aligned} \tilde{ds}^2 &= -(dT')^2 + (dR')^2 \\ -\pi/2 &< T', R' < \pi/2 \end{aligned} \quad (3.33)$$

Having found these coordinates, we can now draw the conformal diagram for the static BTZ Black Hole. It will look like the Schwarzschild Black Hole near the event horizon, but will have the same structure at conformal infinity as  $AdS_3$ :

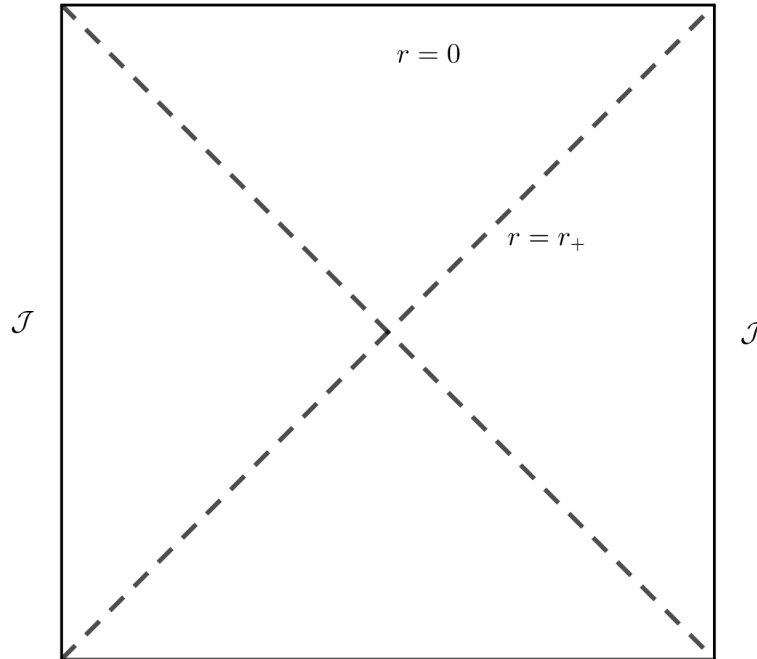


Figure 7: The conformal diagram for the static BTZ black hole. The past and future event horizons are again located at  $r = r_+$ . In this diagram, we now see that the spacetime is asymptotically  $AdS_3$ .

### 3.2 Singularities

As we have already seen in the previous subsection, the apparent singularities at the inner and outer horizon are coordinate dependent singularities, as is also the case for black hole solutions in (3+1) dimensions. Therefore, one would expect the curvature to stay finite on the horizons. In order to check this, and to identify any other potential curvature singularities of the BTZ black hole, we can compute the **curvature invariant**  $R_{ijkl} R^{ijkl}$ . Using the expression we obtained in section 1.3, for the Riemann tensor associated with vacuum solutions to Einstein's Equations, we find that:

$$R_{ijkl} R^{ijkl} = \Lambda^2 (g_{\rho\mu} g_{\nu\sigma} - g_{\rho\nu} g_{\mu\sigma}) (g^{\rho\mu} g^{\nu\sigma} - g^{\rho\nu} g^{\mu\sigma}) = 12 \Lambda^2 \quad (3.34)$$

It is now evident, that the BTZ black hole has no curvature singularities anywhere. This is very different from black holes in (3+1) dimensions, which all possess some kind of curvature singularity in their interior. Although the BTZ black hole possess no curvature singularities, another complication arises if we try to extend the spacetime to  $r^2 < 0$ ; the emergence of **closed time-like curves**. This is most easily seen by performing the following change of coordinate:

$$\tilde{r} = r^2 \quad \Rightarrow \quad d\tilde{r} = 2r dr \quad \Rightarrow \quad dr^2 = \frac{1}{4\tilde{r}} d\tilde{r}^2 \quad (3.35)$$

With this change of coordinate, the static BTZ metric now takes on the following form:

$$ds^2 = - \left[ -M + \frac{\tilde{r}}{\ell^2} \right] dt^2 + \frac{1}{4\tilde{r}} \left[ -M + \frac{\tilde{r}}{\ell^2} \right]^{-1} d\tilde{r}^2 + \tilde{r} d\phi^2 \quad (3.36)$$

If we now extend the range of  $\tilde{r}$  such that  $\tilde{r} \in (-\infty, \infty)$ , it is now clear that for example curves of constant  $t$  and  $\tilde{r}$  become time-like for  $\tilde{r} < 0$ . Because  $\phi$  is compact with  $\phi \sim \phi + 2\pi$ , these curves can always be chosen to be closed. Because of the existence of closed time-like curves in the region  $\tilde{r} < 0$ , this part of the spacetime is usually excluded from the rest of the BTZ spacetime, and  $\tilde{r} = 0$  is called a **causal singularity** of the spacetime. This rather exotic causal singularity at  $\tilde{r} = 0$  will in fact become a **conical singularity** whenever the event horizon at  $r_+^2$  lies in the region of negative  $\tilde{r}$ . Because  $r_+^2 = \ell^2 M$ , this happens when  $M < 0$ . To see this, we now perform the following change of coordinate:

$$\rho = \frac{1}{\mu^2} \sinh^{-1} \left( \frac{r}{\mu \ell} \right) \quad , \quad \mu^2 := -M \quad (3.37)$$

We can now express  $r^2$  and  $f^2(r)$  in terms of the new radial coordinate  $\rho$ :

$$f^2(r) = \mu^2 + \frac{r^2}{\ell^2} = \mu^2 \cosh^2(\rho \mu^2) \quad , \quad r^2 = \ell^2 \mu^2 \sinh^2(\rho \mu^2) \quad (3.38)$$

In terms of  $\rho$ , the static BTZ metric (3.3), now takes the following form:

$$ds^2 = -\mu^2 \cosh^2(\rho \mu^2) dt^2 + d\rho^2 + \ell^2 \mu^2 \sinh^2(\rho \mu^2) d\phi^2 \quad (3.39)$$

Close to  $r = 0 \Leftrightarrow \rho = 0$ , the metric now takes the following approximate form to leading order in  $\rho$ :

$$ds^2 \approx -\mu^2 dt^2 + d\rho^2 + \ell^2 \rho^2 d\tilde{\phi}^2 \quad , \quad \tilde{\phi} \in (0, 2\pi\mu^2) \quad (3.40)$$

It is now manifestly clear, that the static BTZ spacetime for  $M < 0$  has a conical singularity in the  $(\rho, \phi)$ -plane, at  $\rho = 0$ , with a deficit angle of  $\alpha = 1 - \mu^2$ . As mentioned earlier, the event horizon at  $r_+^2 = \ell^2 M$  lies beyond the conical singularity at  $r = 0$ , and it is thus a **naked singularity**. As discussed in [3], these same phenomena happen for the general BTZ spacetime when  $J^2 > \ell^2 M^2$ .

## 4 Quantum fields on fixed BTZ background

In the previous section, we found that the causal structure of the static BTZ spacetime is very similar to that of the Schwarzschild spacetime (*see figures (3) and (7) in sections 1 and 3, for comparison*). This leads us to suspect that quantum fields defined on the right patch of the maximally extended BTZ spacetime, might be at non-zero temperature. This turns out to be the case which we will show in this section, by analysing the BTZ **Green's functions** defined on the right patch, following closely the derivation found in appendix A of [4]. We shall use a **conformally coupled** scalar field, as this will make the computation of the Green's functions considerably easier. Furthermore, we will in this discussion ignore any effects of **back-reaction** on the geometry, induced by the energy-momentum tensor of the scalar field. For an extensive discussion of these effects, see [4].

### 4.1 KMS condition and the two-point function

Before we compute the Green's functions on the BTZ spacetime, let us first briefly discuss how to identify a quantum state at non-zero temperature. From quantum statistical mechanics, we know that the expectation value of an operator  $A$  with respect to the thermal equilibrium state, is given by:

$$\langle A \rangle_\beta = \frac{1}{Z} \text{Tr}[e^{-\beta H} A] \quad , \quad Z = \text{Tr}[e^{-\beta H}] \quad (4.1)$$

Where  $H$  is the Hamiltonian operator of the quantum system, and  $\beta$  is its inverse temperature. The Hamiltonian is also responsible for defining the time-evolution of any operator  $A$  (*we are evidently working in the **Heisenberg picture***):

$$A_t = e^{itH} A e^{-itH} \quad (4.2)$$

The expression (4.1) for thermal expectation is well defined for systems with finite number of degrees of freedom. However, for systems with a continuous spectrum, such as free scalar fields, the partition function  $Z$  tends to diverge, rendering (4.1) practically unusable. To work around this inconvenience, we can combine the expressions (4.1) and (4.2) to form what is known as the **KMS condition**:

$$\langle A_{t-i\beta} B \rangle_\beta = \frac{1}{Z} \text{Tr}[e^{-\beta H} (e^{\beta H} A_t e^{-\beta H}) B] = \frac{1}{Z} \text{Tr}[e^{-\beta H} B A_t] = \langle B A_t \rangle_\beta \quad (4.3)$$

A state that satisfies the KMS condition for all operators  $A$  and  $B$ , is then said to be a thermal KMS state. It can be shown, that the KMS condition (4.3) is equivalent to (4.1) for systems with finite degrees of freedom. To further aid us identify thermal states of free scalar fields, we need to investigate how the KMS condition affects the properties of certain objects defined from the field operators  $\phi(x)$ . To do so, we first introduce the two **Wightman functions**, defined as follow:

$$G^+(x, x') = \langle 0 | \phi(x) \phi(x') | 0 \rangle \quad , \quad G^-(x, x') = \langle 0 | \phi(x') \phi(x) | 0 \rangle \quad (4.4)$$

Now, in order for any notion of thermal equilibrium to exist, the spacetime on which the scalar field theory is defined, must be static. Thus, it must admit a time-like Killing vector  $\partial_t$ , with an associated foliation of the spacetime  $(t, \mathbf{x})$ . The existence of the Killing vector  $\partial_t$  also implies that the Wightman functions only depend on time differences  $\Delta t$ . We can now use the KMS condition to relate the two Wightman functions. The result is the following:

$$G_\beta^+(\Delta t - i\beta; \mathbf{x}, \mathbf{x}') = \langle \phi_{t-i\beta}(\mathbf{x}) \phi_{t'}(\mathbf{x}') \rangle_\beta = \langle \phi_{t'}(\mathbf{x}') \phi_t(\mathbf{x}) \rangle_\beta = G_\beta^-(\Delta t; \mathbf{x}, \mathbf{x}') \quad (4.5)$$

We can slightly rewrite the above, by noting that  $G^-(x, x') = G^+(x', x)$ . Written in terms of the foliation  $(t, \mathbf{x})$ , this becomes  $G_\beta^-(\Delta t; \mathbf{x}, \mathbf{x}') = G_\beta^+(-\Delta t; \mathbf{x}', \mathbf{x})$ . We thus arrive at the following relation:

$$\boxed{G_\beta^+(\Delta t - i\beta; \mathbf{x}, \mathbf{x}') = G_\beta^+(-\Delta t; \mathbf{x}', \mathbf{x})} \quad (4.6)$$

This relation is the one that will finally reveal, that observers at fixed distance from the event horizon of the static BTZ black hole experience a non-zero temperature, once we have computed  $G^+(x, x')$ .



### 4.1.1 Computing the AdS Green's functions

In order to compute the Wightman function  $G^+(x, x')$  on  $AdS_3$  we will now make use of the fact that a coordinate system can be chosen on  $AdS_3$ , such that the metric takes the following simple form:

$$ds_A^2 = \Omega^2 ds_E^2 \quad , \quad ds_E^2 = -d\lambda^2 + d\chi^2 + \sin^2 \chi d\theta^2 \quad , \quad \Omega = \frac{\ell}{\cos \chi} \quad (4.7)$$

$$\lambda \in (-\infty, \infty) \quad , \quad \chi \in \left(0, \frac{\pi}{2}\right) \quad , \quad \theta \in (0, 2\pi)$$

These are the same coordinates (2.34) as we used back in section 2.3 to derive a conformal diagram for  $AdS_3$ . We see that the metric  $ds_A^2$  is conformally related to the metric  $ds_E^2$ , which is the metric of a spacetime known as the **Einstein static universe**. In what follows, all we need to know about the  $ESU$  is that the metrics  $ds_E^2$  and  $ds_A^2$ , are related by the conformal factor  $\Omega$ . We now introduce conformally coupled scalar fields  $\phi_E$  and  $\phi_A$  on the  $ESU$  and  $AdS_3$  respectively. The action for a conformally coupled field is given by:

$$\mathcal{A} = \int_{\mathcal{M}} \sqrt{-g} \left( -\frac{1}{2} g^{\mu\nu} \nabla_\mu \phi \nabla_\nu \phi - \frac{1}{2} \xi R \phi^2 \right) \quad (4.8)$$

Where  $\xi = \frac{(n-2)}{4(n-1)}$ . For  $n = 3$ , the equation of motion associated with the above action is given by:

$$\left( \square - \frac{1}{8} R \right) \phi = \left( g^{\mu\nu} \nabla_\mu \nabla_\nu - \frac{1}{8} R \right) \phi = 0 \quad (4.9)$$

It can be shown, that under the conformal transformation  $ds_E^2 \rightarrow ds_A^2 = \Omega^2 ds_E^2$ , the field equation (4.9) transforms in the following way, due to  $\phi$  being a conformally coupled field:

$$\left( \square_E - \frac{1}{8} R_E \right) \phi_E = 0 \quad \rightarrow \quad \left( \square_A - \frac{1}{8} R_A \right) \phi_A = 0 \quad , \quad \phi_A = \Omega^{-\frac{1}{2}} \phi_E \quad (4.10)$$

Where  $R_E = 2$  is the Ricci scalar of the  $ESU$ ,  $R_A = 6\ell^{-2}$  is the Ricci scalar of  $AdS_3$ . Thus, any solution to the field equation (4.9) on the  $ESU$ , will be related to a solution of (4.9) on  $AdS_3$  by the factor  $\Omega^{-\frac{1}{2}}$ . We now proceed to look for a complete set of modes  $\psi_E$ , of equation (4.9) on the  $ESU$ :

$$\left( \square_E - \frac{1}{4} \right) \psi_E = \left( -\partial_\lambda^2 + \partial_\chi^2 + \frac{\cos \chi}{\sin \chi} \partial_\chi + \frac{1}{\sin^2 \chi} \partial_\theta^2 - \frac{1}{4} \right) \psi_E \quad (4.11)$$

To solve the above equation of motion, we propose the following separable ansatz for the modes  $\psi_E$ :

$$\phi_E(\lambda, \chi, \theta) = e^{-i\omega\lambda} f(\chi, \theta) \quad (4.12)$$

Using the above ansatz, the field equation (4.11) now takes the following form:

$$\omega^2 f(\chi, \theta) + \partial_\chi^2 f(\chi, \theta) + \frac{\cos \chi}{\sin \chi} \partial_\chi f(\chi, \theta) + \frac{1}{\sin^2 \chi} \partial_\theta^2 f(\chi, \theta) - \frac{1}{4} f(\chi, \theta) = 0 \quad (4.13)$$

Further algebraic manipulations yields, that the above expression can be brought to the form:

$$(\sin \chi \partial_\chi (\sin \chi \partial_\chi) + \partial_\theta^2) f(\chi, \theta) = \left( \frac{1}{4} - \omega^2 \right) \sin^2 \chi f(\chi, \theta) \quad (4.14)$$

We notice that the above equation is exactly the one defining the **spherical harmonics**  $Y_l^m(\chi, \theta)$ , if we require that the following relation between  $l$  and  $\omega$  holds true:

$$\frac{1}{4} - \omega^2 = -l(l+1) \quad \Rightarrow \quad \omega^2 = l^2 + l + \frac{1}{4} = \left( l + \frac{1}{2} \right)^2 \quad \Rightarrow \quad \omega = l + \frac{1}{2} \quad (4.15)$$

Thus, we see that the functions  $f(\chi, \theta) = Y_l^m(\chi, \theta)$  solve (4.14), and the modes  $\psi_E$  take the form:

$$\psi_E(\lambda, \chi, \theta) = N_{lm} e^{-i(l+\frac{1}{2})\lambda} Y_l^m(\chi, \theta) \quad (4.16)$$

Where  $N_{lm}$  is just any constant. Using the relation (4.10), we find that the corresponding modes  $\psi_A$  on  $AdS_3$  are given by the following:

$$\psi_A(\lambda, \chi, \theta) = \sqrt{\frac{\cos \chi}{\ell}} N_{lm} e^{-i(l+\frac{1}{2})\lambda} Y_l^m(\chi, \theta) \quad (4.17)$$

We can now define a hypersurface-invariant inner product on the space of solutions of (4.9), such that:

$$(f, g) = -i \int_{\Sigma} d^2x \sqrt{\gamma} (f \nabla_{\mu} g^* - g^* \nabla_{\mu} f) n^{\mu} \quad (4.18)$$

Where  $n^{\mu}$  is the unit normal vector of  $\Sigma$ , and  $\gamma_{ij}$  is the induced metric on  $\Sigma$ . With respect to this inner product, we find that the modes (4.16) and their complex conjugates, are an orthonormal set of modes, if we require that  $N_{lm} = (2l+1)^{-\frac{1}{2}}$ :

$$(\psi_{lm}, \psi_{l'm'}^*) = 0 \quad , \quad (\psi_{lm}, \psi_{l'm'}) = \delta_{mm'} \delta_{ll'} N_l \quad , \quad (\psi_{lm}^*, \psi_{l'm'}^*) = -\delta_{mm'} \delta_{ll'} N_l \quad (4.19)$$

We can expand the field operator  $\phi_E(x)$  in these positive and negative frequency modes, such that:

$$\phi_E(x) = \sum_{m,l} \psi_{lm}(x) a_{lm} + \psi_{lm}^*(x) a_{lm}^{\dagger} \quad (4.20)$$

Where  $a_{lm}^{\dagger}$  and  $a_{lm}$  are the creation and annihilation operators, associated with the modes  $\psi_{lm}$ . The Green's function  $G_E^+(x, x')$  can now be rewritten in terms of the above mode expansion for  $\phi_E$ :

$$G_E^+(x, x') = \langle 0 | \phi(x) \phi(x') | 0 \rangle = \sum_{m,l} \psi_{lm}^E(x) \psi_{lm}^{*E}(x') \quad (4.21)$$

Where as usual, we define the ground state  $|0\rangle$  such that  $a_{lm} |0\rangle = 0$ ,  $\forall l, m$ . We now insert the expression for the  $ESU$  modes (eq 4.16), into the Green's function expansion (eq 4.21). Making use of the following identities for the spherical harmonics  $Y_m^l$ :

$$(Y_m^l)^* = (-1)^m Y_{-m}^l \quad (4.22)$$

$$\sum_{m=-l}^l (-1)^m Y_m^l(\chi, \theta) Y_m^l(\chi', \theta') = \frac{2l+1}{4\pi} P_l(\cos \alpha) \quad (4.23)$$

$$\cos \alpha = \cos \chi \cos \chi' + \sin \chi \sin \chi' \cos(\Delta\theta) \quad (4.24)$$

Where  $P_l$  are the **Legendre polynomials**, and  $\alpha$  is the angle between  $(\chi, \theta)$  and  $(\chi', \theta')$ . This all leads to the following expression for the Green's Function  $G_E^+(x, x')$ :

$$G_E^+ = \frac{1}{4\pi} e^{-\frac{i}{2}\Delta\lambda} \sum_{l=0}^{\infty} e^{-il\Delta\lambda} P_l(\cos \alpha) \quad (4.25)$$

Now, we use the following property of the Legendre polynomials  $P_l$  to evaluate the infinite sum:

$$\sum_{n=0}^{\infty} P_n(y) z^n = (1 - 2yz + z^2)^{-\frac{1}{2}} \quad (4.26)$$

Where in our case,  $z = e^{-i(\Delta\lambda - i\epsilon)}$  and  $y = \cos \alpha$ . We also add a small negative imaginary part to  $\Delta\lambda$  to ensure that the above sum does not diverge. Now, we can make use of the fact that the modes on the  $ESU$  and  $AdS_3$  are related by (4.10), to arrive at an expression for the Green's function  $G_A^+(x, x')$ :

$$\begin{aligned}
G_A^+(x, x') &= \frac{\sqrt{\cos \chi \cos \chi'}}{4\pi \ell} e^{-\frac{i}{2}(\Delta\lambda - i\epsilon)} \left(1 - 2 \cos \alpha e^{-i(\Delta\lambda - i\epsilon)} + e^{-2i(\Delta\lambda - i\epsilon)}\right)^{-\frac{1}{2}} \\
&= \frac{1}{4\pi \ell} \left(e^{i(\Delta\lambda - i\epsilon)} - 2 \cos \alpha + e^{-i(\Delta\lambda - i\epsilon)}\right)^{-\frac{1}{2}} = \frac{1}{4\sqrt{2\pi} \ell} (\cos(\Delta\lambda - i\epsilon) - \cos \alpha)^{-\frac{1}{2}} \\
&= \frac{1}{4\sqrt{2\pi} \ell} (\cos(\Delta\lambda - i\epsilon) \sec \chi \sec \chi' - 1 - \tan \chi \tan \chi' \cos \Delta\theta)^{-\frac{1}{2}} \quad (4.27)
\end{aligned}$$

If we now call the above Green's function  $G_{1,A}^+$ , we can define another Green's function on  $AdS_3$  as  $G_{2,A}^+(x, x') = G_{1,A}^+(\bar{x}, x)$ , where  $\bar{x} = (\lambda, \pi - \chi, \theta)$ . The two Green's functions will then be given by:

$$\begin{aligned}
G_{1,A}^+(x, x') &= \frac{1}{4\sqrt{2\pi} \ell} (\cos(\Delta\lambda - i\epsilon) \sec \chi \sec \chi' - 1 - \tan \chi \tan \chi' \cos \Delta\theta)^{-\frac{1}{2}} \\
G_{2,A}^+(x, x') &= \frac{1}{4\sqrt{2\pi} \ell} (\cos(\Delta\lambda - i\epsilon) \sec \chi \sec \chi' + 1 - \tan \chi \tan \chi' \cos \Delta\theta)^{-\frac{1}{2}} \quad (4.28)
\end{aligned}$$

Since  $AdS_3$  is globally non-hyperbolic, it is necessary to impose boundary conditions on the field operators  $\phi_A(x)$  at infinity ( $\chi = \frac{\pi}{2}$ ), to insure a well behaved quantum field theory on  $AdS_3$ . For a discussion of this procedure, see [4]. It turns out that imposing the appropriated boundary conditions on  $\phi_A(x)$ , in turn leads to the following Greens's functions:

$$G_{A\pm}^+ = G_{1,A}^+ \pm G_{2,A}^+ \quad , \quad G_{A-}^+ \left(\chi = \frac{\pi}{2}\right) = 0 \quad , \quad \partial_\chi G_{A+}^+ \left(\chi = \frac{\pi}{2}\right) = 0 \quad (4.29)$$

Thus,  $G_{A-}^+$  have **Neumann boundary conditions**, while  $G_{A+}^+$  have **Dirichlet boundary conditions**.

#### 4.1.2 Computing the BTZ Green's functions

Back in section 2.3, we found that it is possible to cover a portion of  $AdS_3$  with a set of coordinates  $(t, r, \phi)$  defined by (B.1), (B.2) and (B.3). In the case of the static BTZ spacetime, we let  $r_- \rightarrow 0$ , and use only (B.1) and (B.2). As we are only interested in investigating the properties of the Green's functions for observers outside the event horizon, we will only use the coordinates given by (B.1). The Green's functions (4.28) in coordinates  $(t, r, \phi)$  are then given by:

$$\begin{aligned}
G_{1,A}^+(x, x') &= \frac{1}{4\sqrt{2\pi} \ell} \left[ \frac{r r'}{r_+^2} \cosh \left( \frac{r_+ \Delta\phi}{\ell} \right) - 1 - \frac{\zeta(r, r')}{r_+^2} \cosh \left( \frac{r_+ (\Delta t - i\epsilon)}{\ell^2} \right) \right]^{-\frac{1}{2}} \\
G_{2,A}^+(x, x') &= \frac{1}{4\sqrt{2\pi} \ell} \left[ \frac{r r'}{r_+^2} \cosh \left( \frac{r_+ \Delta\phi}{\ell} \right) + 1 - \frac{\zeta(r, r')}{r_+^2} \cosh \left( \frac{r_+ (\Delta t - i\epsilon)}{\ell^2} \right) \right]^{-\frac{1}{2}} \quad (4.30) \\
\zeta(r, r') &= (r^2 - r_+^2)^{\frac{1}{2}} (r'^2 - r_+^2)^{\frac{1}{2}}
\end{aligned}$$

We can now use the method of images to derive the Green's Functions on the BTZ spacetime from the Green's Functions on  $AdS_3$ . Because BTZ can be constructed from  $AdS_3$  by making the identification  $\phi = \phi + 2\pi n$ , we must require that the Green's functions on BTZ are periodic in  $\phi$ . To achieve this, we construct them as:

$$\begin{aligned}
G_1^+(x, x') &= \frac{1}{4\sqrt{2\pi} \ell} \sum_{n=-\infty}^{\infty} \left[ \frac{r r'}{r_+^2} \cosh \left( \frac{r_+ (\Delta\phi + 2\pi n)}{\ell} \right) - 1 - \frac{\zeta(r, r')}{r_+^2} \cosh \left( \frac{r_+ (\Delta t - i\epsilon)}{\ell^2} \right) \right]^{-\frac{1}{2}} \\
G_2^+(x, x') &= \frac{1}{4\sqrt{2\pi} \ell} \sum_{n=-\infty}^{\infty} \left[ \frac{r r'}{r_+^2} \cosh \left( \frac{r_+ (\Delta\phi + 2\pi n)}{\ell} \right) + 1 - \frac{\zeta(r, r')}{r_+^2} \cosh \left( \frac{r_+ (\Delta t - i\epsilon)}{\ell^2} \right) \right]^{-\frac{1}{2}} \quad (4.31)
\end{aligned}$$

### 4.1.3 The KMS condition

We will now proceed to show that the Green's functions defined by (4.31) obey the KMS condition (4.6). We will do this by showing that each term in the sums (4.31) obeys the KMS condition separately. For a typical term in the sum in (4.3) there is a singularity where the square root vanishes, which is to say when:

$$0 = \frac{r r'}{r_+^2} \cosh \left( \frac{r_+(\Delta\phi + 2\pi n)}{\ell} \right) \pm 1 - \frac{\zeta(r, r')}{r_+^2} \cosh \left( \frac{r_+(\Delta t - i\epsilon)}{\ell^2} \right) \quad (4.32)$$

Assuming that  $\Delta t$  takes on the form  $\Delta t = i\epsilon + i p \beta \pm \Delta t_n^0$  where  $p$  is any integer:

$$\frac{\zeta(r, r')}{r_+^2} \cosh \left( \frac{r_+}{\ell^2} (i p \beta \pm \Delta \tau_n^0) \right) = \frac{r r'}{r_+^2} \cosh \left( \frac{r_+(\Delta\phi + 2\pi n)}{\ell} \right) \pm 1 \quad (4.33)$$

We know that  $\cosh$  is periodic with period  $2\pi i$ , so we see that if we choose  $\beta^{-1} = \frac{r_+}{2\pi\ell^2}$ , we get:

$$\frac{\zeta(r, r')}{r_+^2} \cosh \left( \frac{r_+ \Delta \tau_n^0}{\ell^2} \right) = \frac{r r'}{r_+^2} \cosh \left( \frac{r_+(\Delta\phi + 2\pi n)}{\ell} \right) \pm 1 \quad (4.34)$$

Which serves as a definition of  $\Delta \tau_n^0$  that ensures that all points such that  $\Delta \tau = i\epsilon + \frac{i}{T}p \pm \Delta \tau_n^0$  are singular and we therefore make the square root branch cuts  $(\Delta \tau_n^0 + i\epsilon + \frac{i}{T}p \rightarrow \infty + i\epsilon + \frac{i}{T}p)$  and  $(-\Delta \tau_n^0 + i\epsilon + \frac{i}{T}p \rightarrow -\infty + i\epsilon + \frac{i}{T}p)$ . In the regions without any branch cuts, it is easy to see that:

$$G^+(\Delta t - i\beta; \mathbf{x}, \mathbf{x}') = G^+(\Delta t; \mathbf{x}, \mathbf{x}') = G^+(-\Delta t; \mathbf{x}', \mathbf{x}) \quad (4.35)$$

If however we are in a region with a branch cut, we must be a little more careful. Going through a branch cut gives a minus, so we see that:

$$G^+(\Delta t - i\beta; \mathbf{x}, \mathbf{x}') = -G^+(\Delta t; \mathbf{x}, \mathbf{x}') \quad (4.36)$$

It is shown in [4] that  $-G^+(-\Delta t; \mathbf{x}, \mathbf{x}') = G^+(\Delta t; \mathbf{x}, \mathbf{x}')$ , which we can use to see that

$$G^+(\Delta t - i\beta; \mathbf{x}, \mathbf{x}') = G^+(-\Delta t; \mathbf{x}', \mathbf{x}) \quad (4.37)$$

Which is exactly the KMS condition (4.6). This leads us to conclude that the Green's functions are thermal and that we can associate a the following temperature with the static BTZ black hole:

$$\boxed{T = \beta^{-1} = \frac{r_+}{2\pi\ell^2}} \quad (4.38)$$

## 5 Conclusion

We have seen that the metric for the BTZ Black Hole can be derived from the requirements that it is stationary and circularly symmetric, which is the same as saying it has two killing vectors  $\partial_\phi$  and  $\partial_t$ . Because the spacetime is (2+1) dimensional, it has been shown that it must be locally maximally symmetric. Additionally, it has been shown that the BTZ spacetime can be constructed from the  $\text{AdS}_3$  spacetime with the identification  $\phi \sim \phi + 2\pi$ . Through an analysis of the metric and the conformal diagram for the spacetime, we see that the causal structure of the BTZ Black Hole is that of the Schwarzschild Black Hole near the horizon and the  $\text{AdS}_3$  near infinity. Unlike in the Schwarzschild solution, the point at  $r = 0$  has been shown to not possess a curvature singularity. Instead, it is of a more exotic form called a causal singularity for  $M > 0$  and a conical singularity for  $M < 0$ .

Through finding thermal Green's Functions for a conformally coupled scalar field on the BTZ Black Hole background, we have shown that we can associate a temperature of  $T = \frac{r_+}{2\pi\ell^2}$  with the static BTZ Black Hole. This result calls for further research in the evaporation of a BTZ Black Hole.

## Bibliographical notes

This thesis is the product of a 4 month reading course on General Relativity following the textbook by Sean Carroll [1] and going through:

- Chapter 1: Special Relativity and Flat Spacetime
- Chapter 2: Manifolds
- Chapter 3: Curvature
- Chapter 4: Gravitation
- Chapter 5: The Schwarzschild Solution
- Chapter 6: More General Black Holes
- Chapter 9: Quantum Field Theory in Curved Spacetime

In the end of the course, we touched upon different aspect of Quantum Field Theory on curved spacetimes, specifically on the (2+1)-dimensional black hole, following the articles:

- Black Hole Thermodynamics [2]
- The (2+1)-Dimensional Black Hole [3]
- Scalar Field Quantization on the 2+1 Dimensional Black Hole Background [4]

## References

- [1] S. Carroll. *Spacetime and Geometry: an introduction to general relativity*. ISBN: 0-8053-8732-3
- [2] Simon F. Ross *Black hole thermodynamics*. <http://arXiv.org/abs/hep-th/0502195v2>
- [3] S. Carlip *The (2+1)-Dimensional Black Hole*. <http://arXiv.org/abs/gr-qc/9506079v1>
- [4] G. Lifschytz and M. Ortiz *Scalar Field Quantization on the 2+1 Dimensional Black Hole Background*. <http://arXiv.org/abs/gr-qc/9310008>
- [5] Robert M. Wald *General Relativity*. ISBN: 0-226-87033-2

# A The basics of General Relativity

In this appendix we provide a short review some of the basic aspects of general relativity. It is structured as a set of definitions as they are given in [1]; readers new to the subject should consult a text book on the subject such as [1]. We shall assume that the reader is familiar with the concept of tensors and understands that spacetime is a manifold.

## A.1 Differential Forms

A differential p-form is an antisymmetric (0,p)-tensor. It is easy to show that at any point on a n-dimensional manifold there are

$$\frac{n!}{p!(n-p)!} \quad (\text{A.1})$$

linearly independent p-forms. It is possible to define a wedge product between two manifolds  $A$  and  $B$ . If  $A$  is a p-form and  $B$  a q-form, then the wedge product between them will be a (p+q)-form given by:

$$(A \wedge B)_{\mu_1 \dots \mu_{p+q}} = \frac{p! q!}{(p+q)!} B_{[\mu_1 \dots \mu_q} A_{\mu_{q+1} \dots \mu_{q+p}]} \quad (\text{A.2})$$

The usefulness of differential forms and the reason they have their own name is that there exists a sensible concept of differentiation called the exterior derivative, which makes a (p+1)-form field out of a p-form field:

$$(dA)_{\mu_1 \dots \mu_{p+1}} = \partial_{[\mu_1} A_{\mu_2 \dots \mu_{p+1}]} \quad (\text{A.3})$$

## A.2 The metric

The metric tensor is a symmetric (0,2) tensor usually denoted  $g_{\mu\nu}$ . It is nondegenerate, meaning that the determinant does not vanish, which allows us to define the inverse metric  $g^{\mu\nu} g_{\nu\sigma} = g_{\mu\rho} g^{\rho\sigma} = \delta^\mu_\sigma$ . The metric is generally what we use to lower or raise indices, e.g. for a tensor  $A^\mu_{\nu\sigma}$  we define  $A^{\mu\nu}{}_\sigma = g^{\nu\rho} A^\mu_{\rho\sigma}$ . Furthermore, the metric is used to measure path lengths through the line element  $ds^2 = g_{\mu\nu} dx^\mu dx^\nu$ . Because  $dx^\mu$  is just a basis dual vector, we shall use  $g_{\mu\nu}$  and  $ds^2$  interchangeably. An example of a metric is the classic 3-dimensional Euclidean space with coordinates  $(x, y, z)$  on which the metric is written:

$$ds^2 = dx^2 + dy^2 + dz^2 \quad (\text{A.4})$$

## A.3 Covariant Derivatives and Connections

In general the partial derivative of a tensor is not itself a tensor. Therefore we would like an operator that reduces to the partial derivative on a flat spacetime, but which itself is a proper tensor. It can be shown that we can define the covariant derivative of a vector (a similar definition can be given for any tensor) by

$$\nabla_\mu V^\nu = \partial_\mu V^\nu + \Gamma^\nu_{\mu\sigma} V^\sigma \quad (\text{A.5})$$

where  $\Gamma^\nu_{\mu\sigma}$  is called a connection and is just a matrix that makes sure the covariant derivative is indeed covariant. The connection will not itself transform like a tensor, but that is to be expected, since it is defined such that it together with the partial derivative forms a tensor. We can require of the connection that it is

$$\text{Torsion free:} \quad \Gamma^\nu_{\mu\sigma} = \Gamma^\nu_{(\mu\sigma)} \quad (\text{A.6})$$

$$\text{Metric compatible:} \quad \nabla_\sigma g_{\mu\nu} = 0 \quad (\text{A.7})$$

Given a metric, it can be shown that this defines a unique connection which we call a Christoffel symbol. This is usually the only connection physicists we are interested in when they do general relativity. The Christoffel symbol can be calculated when the metric is known from the following relation:

$$\Gamma_{\mu\nu}^{\sigma} = \frac{1}{2}g^{\sigma\rho}(\partial_{\mu}g_{\nu\rho} + \partial_{\nu}g_{\rho\mu} - \partial_{\rho}g_{\mu\nu}) \quad (\text{A.8})$$

## A.4 Curvature of the spacetime

All information about the curvature of a spacetime is contained in the (1,3) tensor  $R^{\rho}_{\sigma\mu\nu}$  called the Riemann tensor. This means that if the Riemann tensor vanishes, there exists a set of coordinates in which the metric components are constant (and the opposite is also true). The Riemann tensor is defined from the connections coefficients as:

$$R^{\rho}_{\sigma\mu\nu} = \partial_{\mu}\Gamma_{\nu\sigma}^{\rho} - \partial_{\nu}\Gamma_{\mu\sigma}^{\rho} + \Gamma_{\mu\lambda}^{\rho}\Gamma_{\nu\sigma}^{\lambda} - \Gamma_{\nu\lambda}^{\rho}\Gamma_{\mu\sigma}^{\lambda} \quad (\text{A.9})$$

It is easy to see that the Riemann tensor will be anti-symmetric in its last two indices. If the connection coefficients are the Christoffel symbols (which we shall assume from now on), we can also show that the Riemann tensor with all lower indices  $R_{\rho\sigma\mu\nu}$  is anti-symmetric in the first two indices, symmetric under the swap of the first two indices with the last two and that the anti-symmetric part of the last three indices vanish:

$$R_{\rho\sigma\mu\nu} = -R_{\rho\sigma\nu\mu} \quad , \quad R_{\rho\sigma\mu\nu} = -R_{\sigma\rho\mu\nu} \quad , \quad R_{\rho\sigma\mu\nu} = R_{\mu\nu\rho\sigma} \quad , \quad R_{\rho[\sigma\mu\nu]} = 0 \quad (\text{A.10})$$

From the Riemann tensor we can define the Ricci tensor (which will be symmetric) by contracting two indices:

$$R_{\mu\nu} = R^{\lambda}_{\mu\lambda\nu} \quad (\text{A.11})$$

And from the Ricci tensor we can define the Ricci scalar (also known as curvature scalar) by taking the trace:

$$R = R^{\sigma}_{\sigma} \quad (\text{A.12})$$

A slightly different and less computationally intensive method is described in [5].

## A.5 Geodesics

A geodesic is a path defined as either a path parallel transporting its own tangent vector or a path of minimum distance (/proper time). Geodesics can be found by solving the geodesic equation:

$$\frac{d^2x^{\mu}}{d\lambda^2} + \Gamma_{\rho\sigma}^{\mu} \frac{dx^{\rho}}{d\lambda} \frac{dx^{\sigma}}{d\lambda} = 0 \quad (\text{A.13})$$

Geodesics are important because they are the paths followed by unaccelerated particles.

## A.6 Einstein's Equation

Einstein's Equation is a relation between matter and the spacetime and forms the very foundation of general relativity. It is given as:

$$R_{\mu\nu} - \frac{1}{2}Rg_{\mu\nu} + \Lambda g_{\mu\nu} = 8\pi GT_{\mu\nu} \quad (\text{A.14})$$

where  $\Lambda$  is the cosmological constant.

## A.7 Killing vectors and symmetries

Finding solutions to Einstein's Equation can be difficult, so physicists often turn to symmetries for help. In general such a symmetry can be characterized by a Killing vector obeying Killing's equation:

$$p^\mu \nabla_\mu (K_\nu p^\nu) = 0 \tag{A.15}$$

## A.8 Kruskal and Penrose Diagrams

When investigating the causal properties of a spacetime, it is often useful to turn to the Kruskal or Penrose (also known as conformal) diagrams. The Kruskal diagram is simply the maximally extended spacetime shown in Kruskal coordinates, while the Penrose diagram is the same spacetime in a set of compact coordinates, meaning that all of the spacetime can be displayed on a finite area. The Penrose diagram is especially useful for illustrating the properties of the spacetime at the various infinities.



## B BTZ parameterization of AdS3

The BTZ parameterization of AdS<sub>3</sub> for each of the three regions **I**, **II** and **III**:

**I**  $(r_+ < r)$

$$\begin{aligned} X^0 &= \ell \sqrt{\alpha(r)} \cosh \left( \frac{r_+}{\ell} \phi - \frac{r_-}{\ell^2} t \right) \quad , \quad X^1 = \ell \sqrt{\alpha(r) - 1} \sinh \left( \frac{r_+}{\ell^2} t - \frac{r_-}{\ell} \phi \right) \\ X^2 &= \ell \sqrt{\alpha(r)} \sinh \left( \frac{r_+}{\ell} \phi - \frac{r_-}{\ell^2} t \right) \quad , \quad X^3 = \ell \sqrt{\alpha(r) - 1} \cosh \left( \frac{r_+}{\ell^2} t - \frac{r_-}{\ell} \phi \right) \end{aligned} \quad (\text{B.1})$$

**II**  $(r_- < r < r_+)$

$$\begin{aligned} X^0 &= \ell \sqrt{\alpha(r)} \cosh \left( \frac{r_+}{\ell} \phi - \frac{r_-}{\ell^2} t \right) \quad , \quad X^1 = -\ell \sqrt{1 - \alpha(r)} \sinh \left( \frac{r_+}{\ell^2} t - \frac{r_-}{\ell} \phi \right) \\ X^2 &= \ell \sqrt{\alpha(r)} \sinh \left( \frac{r_+}{\ell} \phi - \frac{r_-}{\ell^2} t \right) \quad , \quad X^3 = -\ell \sqrt{1 - \alpha(r)} \cosh \left( \frac{r_+}{\ell^2} t - \frac{r_-}{\ell} \phi \right) \end{aligned} \quad (\text{B.2})$$

**III**  $(0 < r < r_-)$

$$\begin{aligned} X^0 &= \ell \sqrt{-\alpha(r)} \cosh \left( \frac{r_+}{\ell} \phi - \frac{r_-}{\ell^2} t \right) \quad , \quad X^1 = -\ell \sqrt{1 - \alpha(r)} \sinh \left( \frac{r_+}{\ell^2} t - \frac{r_-}{\ell} \phi \right) \\ X^2 &= \ell \sqrt{-\alpha(r)} \sinh \left( \frac{r_+}{\ell} \phi - \frac{r_-}{\ell^2} t \right) \quad , \quad X^3 = -\ell \sqrt{1 - \alpha(r)} \cosh \left( \frac{r_+}{\ell^2} t - \frac{r_-}{\ell} \phi \right) \end{aligned} \quad (\text{B.3})$$

$$\alpha(r) = \frac{r^2 - r_-^2}{r_+^2 - r_-^2}$$